Resource driven community dynamics of NH4+ assimilating and N2O reducing archaea in a temperate paddy soil

Type of article: original article

Resource driven community dynamics of NH_4^+ assimilating and N_2O reducing archaea in a temperate paddy soil

Maria Alexandra Cucu[1,2,3*], Sven Marhan[2], Daniel Said-Pullicino[1], Luisella Celi[1], Ellen Kandeler[2] and Frank Rasche[3]

[1]Rice Agro-ecosystem and Environmental Research Group, Department of Agricultural, Forest and Food Sciences, University of Turin, Italy

[2]Institute of Soil Science and Land Evaluation, Soil Biology Section, University of Hohenheim, Stuttgart, Germany

[3]Institute of Plant Production and Agroecology in the Tropics and Subtropics, University of Hohenheim, Stuttgart, Germany

Running title: Archaeal N cycling in temperate paddy soils

***Corresponding author:**

Dr. Maria Alexandra Cucu

Phone: +39 011 670 8544

Fax: +39 011 670 8692

Email: mariaalexandra.cucu@unito.it

Abstract.

In fertilized paddy soils, the role of resource availability on ammonium (NH_4^+) assimilation and immobilization by archaea requires advanced understanding as this may have considerable implications on subsequent catalytic steps in the soil N cycle including archaeal nitrous oxide (N_2O) reduction. To gain a deeper understanding about these process links, we incubated a temperate paddy soil under submerged conditions with or without straw and fertilized with either ^{15}N-enriched (99 atom% ^{15}N) or non-enriched $(NH_4)_2SO_4$. Notably, a variation in community structure and a higher abundance of archaeal N_2O reductase (*arc-nosZ*) genes in the no straw treatment than in the straw one was observed. This was attributed to NH_4^+ assimilation by N_2O reducing archaea as was further corroborated by a considerable ^{15}N-enrichment of archaeal glutamate dehydrogenase (*gdhA*) genes. Moreover, indications were found that denitrifying archaea controlled their chemotrophic and heterotrophic metabolisms in response to different availabilities of inorganic and organic N and C resources. However, in the presence of straw, bacterial *nosZ* genes may have also contributed to the completion of denitrification. Our results suggested that N assimilation contributed to the last step of archaeal denitrification. Therefore, archaea may play a key role in regulating major N fluxes in fertilized paddy soils, especially in the absence of rice straw.

Keywords: *arc-nosZ* gene; total prokaryotic *nosZ* clade I gene; *gdhA* gene; ^{15}N-DNA-based stable isotope probing**.**

1. Introduction

Fertilized rice paddy soils generally exhibit lower nitrogen (N) recovery rates (30-40%) with respect to upland soils (Cassman et al., 2002). Incorporation of crop residues such as rice straw generally leads to N immobilization (assimilation to sustain their own metabolism) which reduces fertilizer use efficiency to a large extent (Reddy 1982; Eagle et al., 2000; Bird et al., 2001). In previous studies we observed that addition of rice straw induced, in comparison to no straw addition, an 80% increase of immobilization of applied ammonium (NH_4^+) along with a 65% decrease in gaseous N losses (Cucu et al., 2014; Said-Pullicino et al., 2014). On the other hand, incorporation of rice straw in paddies was shown to stimulate N gaseous losses (i.e., N oxide gases and N_2) from soil-plant systems since up to 70% of applied N may be lost through coupled nitrification-denitrification (Cassman et al., 1998; Ghosh and Bhat, 1998; Majumdar, 2013). Significant amounts of nitrous oxide (N_2O), an important greenhouse gas, have been shown to be emitted under aerobic conditions (Zou et al., 2007; Ishii et al., 2011a). To mitigate this climate variation promoting process, it was acknowledged that in continuously submerged paddies complete denitrification via microbial nitrous oxide reduction can act as a considerable sink for N_2O which favors N_2 losses (Davidson et al., 1986; Conrad 1995, 1996; Ferrè et al., 2012).

Both N assimilation and denitrification are mediated by specific microbial communities which are well adapted to the anaerobic conditions of paddy environments (Liesack et al., 2000; Kögel-Knabner et al., 2010). These ecosystems are characterized by a dynamic microbial community in which archaea may predominate over bacteria (Cabello et al., 2004, Rush, 2016), and may also exhibit different metabolic pathways and resource utilization. Denitrification *sensu latu*, as the pathway of nitrate (NO_3^-) respiration, can be associated with dissimilatory and assimilatory branches of microbial metabolism (Zumft, 1997). Under anaerobic conditions, bacterial denitrifiers typically adopt a dissimilatory metabolism for their energy gain (Zumft, 1992), while their potential assimilatory NO_3^- reduction pathway is suppressed when NH_4^+ is the predominant inorganic N form (Rice and Tiedje, 1989; Cabello et al., 2004).

Archaeal denitrifiers can simultaneously perform dissimilatory and assimilatory reactions (Rusch, 2013) by using N not only for energy but also electron sink and detoxification (Zumft, 1997). The gained N is also utilized to build up nitrogenous compounds (e.g., DNA, amino sugars, proteins) (Devêvre and Horwáth, 2001; Nannipieri and Paul, 2009), which ultimately contribute to the soil organic N pool (Kögel-Knabner et al., 2010). However, assimilatory NO_3^- reduction is less frequent than respiratory NO_3^- reduction in the archaeal domain (Martínez-Espinosa et al., 2001). Instead, Cabello et al. (2004) highlighted the importance of the archaeal NH_4^+ assimilation pathway catalyzed by glutamate dehydrogenase (GDH). Encoded by the *gdhA* gene, GDH generally shows a high activity under non-limiting NH_4^+ soil conditions (Bonete et al., 2008). This may be the case for fertilized rice agro-ecosystems characterized by high NH_4^+ availability as a result of mineral N addition and mineralization of organic matter (OM) including freshly applied rice straw (Sahrawat, 2004; Cucu et al., 2014). It needs to be pointed out that NH_4^+ assimilation by archaea in paddy soils requires explicit understanding as this may have considerable implications on subsequent catalytic steps in the soil N cycle including the last step of denitrification (i.e., N_2O reduction). Although N fertilization is recognized as the primary factor influencing denitrification under reduced conditions (Garcia and Tiedje 1982; Nogales et al., 2002; Prieme et al., 2002), the role of rice straw and the interactive effects of available N and C resources on archaeal NH_4^+ assimilation and N_2O reduction remains uncertain.

Compared to bacterial denitrification (Philippot et al., 2002; Henry et al., 2006; Ishii et al., 2011b), only limited knowledge exists about this process in archaea. Likewise, only a few archaeal denitrification genes and related enzymes have been investigated so far (de Vries and Schroder, 2002; Cabello et al., 2004). Moreover, information on the reduction of N_2O to N_2 is only available for very few hypertermophilic and halophilic archaeal species including *Haloferax denitrificans* and *Pyrobaculum aerophilum* (Tomlinson et al., 1986; de Vries and Schroder, 2002). Jones et al. (2013) assigned several archaeal species to *nosZ* groups I and II covering the bacterial and archaeal domains. Recently, Rusch (2013) has introduced a complementary marker for the *arc-nosZ* gene

98 that targets the archaeal N_2O reducing community. The *arc-nosZ* gene is part of the total
99 prokaryotic *nosZ* gene clades I and II. Although a phylogenetic bias based on hypertermophilic and
100 halophilic archaeal sequences has to be taken into account due to limited database information,
101 Rusch (2013) considered the *arc-nosZ* gene marker suitable for the full range of applications
102 targeting archaeal denitrifiers. While the crucial role of archaeal species in methanogenesis and
103 methanotrophy in rice paddies (Fazli et al 2013) is well known, their involvement in denitrification
104 remain less understood.
105 The primary objective of this study was to provide advanced understanding about the role of
106 archaea involved in N assimilation coupled with the final step of denitrification (i.e., N_2O
107 reduction) as a function of C and N resource availability in a temperate paddy soil with no NH_4^+
108 limitation. To achieve this goal, we tested the following hypotheses: i) archaeal N assimilation is
109 controlled by the availability of labile organic C substrates (i.e., rice straw addition); ii) a fraction of
110 the assimilated N is used for proliferation of archaeal community members harboring the *arc-nosZ*
111 gene; iii) in absence of rice straw, the relative contribution of archaea to denitrification is more
112 important than that of their bacterial counterparts.
113
114 **2. Materials and methods**
115 2.1. Incubation experiment
116 Soil was collected from the Ap horizon (0-15 cm) of a long-term field experiment in Vercelli,
117 Northwest Italy (45°17′47″N, 8°25′51″E) in February 2012 before rice straw incorporation. The
118 paddy soil, classified as a Haplic Gleysol (WRB, 2007), has been under continuous single-cropped
119 rice cultivation for the last 30 years. The soil had a pH around 6, a sandy loam texture (7% clay,
120 41% silt, 52% sand) and relatively low contents of organic C and total N (11.6 and 1.1 g kg^{-1},
121 respectively). The amount of clay in conjunction with soil organic matter content accounted for the
122 low cation exchange capacity (CEC = 6.7 cmol $_{(+)}$ kg^{-1}). Further details on soil properties have been
123 previously reported in Cucu et al. (2014) and Said-Pullicino et al. (2014). After manual removal of

124 remaining vegetal residues, field moist soil was homogenized after passing through a 2 mm sieve.
125 Rice straw (*Oryza sativa* L. cv. Sirio CL) was sampled from the same experimental site in October
126 2011 after grain harvest, dried at 40°C and cut into 1 cm segments. Total C and N contents of the
127 rice straw were 400 and 6.6 g kg^{-1} respectively, resulting in a C/N ratio of 61.
128 A laboratory incubation experiment was carried out adopting a setup similar to that described by
129 Cucu et al. (2014). The experimental design consisted of a completely randomized arrangement of
130 soil microcosms incubated under submerged conditions with or without the addition of rice straw
131 (application dose of 4.3 g straw kg^{-1} soil, equivalent to 10 Mg dry weight ha^{-1}). After a pre-
132 incubation period with or without straw addition for 14 days at 50% soil water holding capacity to
133 reestablish the microbial equilibrium, inorganic N (application dose of 56 mg N kg^{-1} soil, equivalent
134 to 130 kg N ha^{-1}, generally applied in the field) was added to the soil samples and immediately
135 submerged under 5 cm of deionized water. Inorganic N was added as ^{15}N-labelled $(NH_4)_2SO_4$ (99
136 atom% ^{15}N) to assess active N assimilatory prokaryotes by stable isotope probing (SIP, see below).
137 A second set of soil samples was treated similarly with non-labeled $(NH_4)_2SO_4$ as control for SIP
138 studies (Buckley et al., 2007b; Neufeld et al., 2007). The experiment was run with six replicates per
139 treatment and time point. Incubation under submerged conditions was carried out for 60 days at
140 25°C in the dark. After 1, 5, 10, 20, 30 and 60 days from fertilizer application, soil microcosms
141 were destructively sampled. The fresh soil sample was immediately used for DNA extraction as
142 well as for inorganic N determination (see bellow). Submergence water was decanted, total volume
143 recorded, filtered at 0.45 μm and used for inorganic N determination. Afterwards, both soil and
144 water samples have been frozen at -20 ˚C for further analysis.
145
146 2.2. Chemical analyses
147 N_2O emissions were monitored daily during the first 4 weeks of incubation. On each measurement
148 day, soil microcosm headspace was sampled twice: immediately and 30 min after closure of the
149 lids. Afterwards the gas sample was transferred into pre-evacuated exetainers (5.9 ml, Labco Ltd.,

Lampeter, UK), and analyzed for N_2O using a gas chromatograph equipped with an electron capture detector (Agilent 7890, Santa Clara, CA, USA). Three standard gases with known concentrations were used for gas flux calibration and calculation. N_2O fluxes were calculated by linear regression as described by Hutchinson and Mossier (1981).

Soil pH was measured potentiometrically in H_2O. Submergence water samples as well as 0.5 M K_2SO_4 soil extracts (1:4 w/v soil-to-extractant ratio) were analyzed for inorganic N (NH_4^+, NO_3^-) (Auto-analyzer 3, Bran & Luebbe, Norderstedt, Germany), total dissolved nitrogen (TDN) and dissolved organic carbon (DOC) after sample acidification (TOC/TN analyzer Multi NC 2100S, Analytic Jena GmbH, Jena, Germany).

2.3. Molecular analyses

2.3.1. DNA extraction

At each time point, total DNA was extracted from each fresh individual replicate soil sample using the FastDNA® Spin kit for soil (MP Biomedicals, Solon, Ohio, USA) according to the manufacturer's instructions. DNA quantification was performed with a NanoDrop ND-2000 (NanoDrop Technologies, Wilmington, DE, USA).

2.3.2. Stable isotope probing

Measurement of ^{15}N-enrichment in DNA extracts

To measure the ^{15}N-enrichment of soil DNA extracts according to España et al. (2011), a tin capsule (Hekatech, Wegberg, Germany) was filled with 10 mg sorbsil (May & Baker, Dagenham, United Kingdom) plus 2 µg of the DNA extracts. Twenty µg N of dissolved unlabeled ammonium sulphate (Roth, Karlsruhe, Germany) were then added to the capsule and dried at 50°C overnight. All DNA samples were analyzed with an elemental analyzer (Euro EA 3000; Hekatech) coupled with an isotope ratio mass spectrometer (DeltaPlus XP, Thermo Scientific, Waltham, USA). ^{15}N-enrichment

of DNA extracts was subsequently calculated by taking into account the isotopic signature of the ammonium sulphate spike.

^{15}N-DNA-based stable isotope probing (SIP) was carried out on samples incubated for 30 days, corresponding to distinct alteration of microbial activity (i.e., ^{15}N enrichment of soil DNA extracts) between "straw" and "no straw" treatments. To reach a high concentration and volume for the further centrifugation, two replicates per DNA samples were pooled together. Finally, four DNA samples were selected for SIP: two with highest ^{15}N label (straw: 6.83 atom% ^{15}N, no straw: 5.02 atom% ^{15}N) and two respective ^{14}N controls. Centrifugation mixtures were prepared by adding 5 mg of DNA diluted in 1 mL gradient buffer (0.1 M Tris, 0.1 M KCl, 1 mM EDTA) to 4.9 ml of a 7.163 M CsCl (Calbiochem/Merck, Darmstadt, Germany) solution. Isopycnic fractionation was performed in 5.1 mL polyallomer centrifuge tube (13×51mm) placed in a Vti 65.2 vertical rotor (both Beckman Coulter, Krefeld, Germany). Tubes were then centrifuged in an Optima™ L-90K ultracentrifuge (Beckman Coulter) was performed with 140,000 × *g* at 20°C for 69 h (España et al., 2011). After centrifugation, each gradient was fractionated into 16 individual fractions (312 µl each) using a syringe pump (NE-1000, New Era Pump Systems, New York, NY, USA). Buoyant density was adjusted prior to centrifugation (AR200 digital refractometer, Reichert, New York, USA) and calculated for each fraction according to Buckley et al. (2007b). SIP fractions were precipitated with 20 µg of glycogen (Roche Diagnostics GmbH, Penzbeg, Germany) and 1 ml of a 30% polyethylene glycol 6000 solution (Carl Roth GmbH, Karlsruhe, Germany), washed (70% ethanol) and suspended in 30 µl of Tris-EDTA buffer (pH 8.0) (Neufeld et al., 2007).

2.3.3. Microbial abundance

Abundance of total bacterial and archaeal communities were done by quantifying the respective 16S rRNA genes (Rasche et al., 2011). Description of primer sets and amplification details used for quantitative PCR are specified in Table 1. Quantification of *nosZ* clade I was performed as described by Henry et al. (2006). The quantification of *arc-nosZ* genes was performed using

201 primers published by Rusch, (2013). Primer accuracy was confirmed (Rusch, personal
202 communication) and preliminary tests (data not shown) were carried out to assess the specificity of
203 the primer set for the studied soil. To confirm the targeted archaeal NH_4^+ assimilation process and
204 the implied labeling success, primers targeting N assimilation in *Methanobrevibacter smithii* by
205 means of the GDH system encoded by the *gdhA* gene were used. *Methanobrevibacter* sp. have been
206 earlier found in paddy soils (Fetzer et al., 1993) and bioreactors (i.e., *Methanobrevibacter* related
207 species), here with potential denitrifying abilities (Chuang et al., 2014)
208 Abundance of bacterial and archaeal 16S rRNA genes and of the three functional genes (i.e., total
209 prokaryotic *nosZ* clade I, *arc-nosZ*, archaeal *gdhA*) was determined by quantitative PCR (qPCR)
210 using a StepOnePlus™ Real-Time PCR System (Applied Biosystems, Foster City, CA, USA) for
211 bulk soil DNA as well as for *gdhA* genes in SIP fractions (Table 1). For standard preparation,
212 amplicons from each target gene were generated, purified (Invisorb Fragment CleanUp, Stratec
213 Molecular GmbH, Berlin, Germany), ligated into the Strata-Clone PCR cloning vector pSC-A
214 (Strataclone PCR Cloning Kit, Agilent Technologies Inc.) and ligation products were transformed
215 into StrataClone SoloPack competent cells (Stratagene). Specificity of clones used as quantitative
216 PCR (qPCR) standards were checked via sequencing at LGC Genomics GmbH (Berlin, Germany)
217 and BLAST analysis. Plasmid DNA was isolated (GenElute™ Plasmid Miniprep Kit, Sigma-
218 Aldrich, St. Louis, MO, USA) from standard clones and quantified as described above.
219 As assessed in preliminary tests and qPCR reaction optimization, each 25 µl qPCR cocktail
220 contained 5 ng DNA (16S rRNA genes) or 10 ng DNA (total prokaryotic *nosZ* clade I and archaeal
221 *arc-nosZ* gene), 1x Power SYBR green master mix (Applied Biosystems), 0.15 µM of each primer
222 (Table 1), 0.25 µl of T4 gene 32 protein (500 µg ml^{-1}, MP Biomedicals). For *gdhA* gene, the 25 µl
223 qPCR cocktail contained 1x FastStart Universal SYBR Green Master (ROX) (Roche), 0.2 µM of
224 each primer (Table 1), 0.625 U Uracil-DNA Glycosylase (Roche) and the DNA template (10 ng
225 from extracted soil DNA, 10 µl DNA from SIP fractions). Each sample was quantified in triplicate
226 across plates, while standards in 10-fold serial dilutions were run in duplicate. The optimal dilution

227 of DNA extracts was tested to compensate any reaction inhibition by organic compounds (e.g.,
228 humic acids) co-extracted during DNA isolations (data not shown). Melting curves of amplicons
229 were generated to ensure that fluorescence signals originated from specific amplicons and not from
230 primer dimers or other artifacts. This was confirmed by checking the amplification products on 1%
231 agarose gel. For quality control, melting curve analyses were performed. Amplification efficiency
232 ranged from 80% (archaeal 16S rRNA, total prokaryotic *nosZ* clade I and *arc-nosZ* genes) to 103%
233 (bacterial 16S rRNA and *gdhA* genes). The slopes were between -3.890 and -3.235 and $R^2 \geq 0.98$.
234 Gene copy numbers were calculated with StepOne™ software version 2.2 (Applied Biosystems).
235 The data were normalized and presented in figures as copies g^{-1} dry soil.
236 To determine the relative abundance of *arc-nosZ* gene with respect to the total prokaryotic *nosZ*
237 gene clade I, the *arc-nosZ* to *nosZ* gene abundance ratio was calculated. Values > 0.5 indicate a
238 higher relative abundance of archaea with respect to their bacterial counterparts within total
239 prokaryotic *nosZ* clade I.
240
241 2.3.4. Microbial community structure
242 The community structure of archaeal 16S rRNA, total prokaryotic *nosZ* clade I, and archaeal *arc-*
243 *nosZ* genes in bulk DNA soil, as well as in SIP fractions (total prokaryotic *nosZ* clade I and *arc-*
244 *nosZ* genes) was studied by terminal restriction fragment length polymorphism (T-RFLP) analysis.
245 Description of primer sets, PCR ingredients and amplification details used for T-RFLP analysis are
246 specified in Table 2. Prior to digestion, all genes were amplified using PCR cocktails and
247 amplification according to the details described in Table 2. For T-RFLP analysis, each forward
248 primer was labeled with the fluorescent dye 6-FAM. Replicate amplicons were pooled, purified
249 (Sephadex G-50, GE Healthcare Biosciences, Waukesha, WI, USA) according to Rasche et al.
250 (2006), and 200 ng of each amplicon were digested with 5 U *Alu*I (archaeal 16S rRNA; New
251 England Biolabs (NEB) Inc., Ipswich, MA, USA), overnight at 37°C (Rasche et al., 2011). For the
252 digestion of *nosZ* and *arc-nosZ* gene amplicons, several restriction enzymes and their combinations

253 were tested (data not shown). Finally, 10 U HpyCH4IV (total prokaryotic *nosZ* clade I; NEB) and a
254 10 U cocktail of *Alu*I, *Rsa*I, and HpyCH4IV (*arc-nosZ*; NEB) revealed representative T-RFLP
255 fingerprints of both genes. Prior to T-RFLP analysis, digests were purified with Sephadex™ G-50
256 (Rasche et al., 2006) and a 2 µl aliquot was mixed with 17.75 µl HiDi formamide (Applied
257 Biosystems) and 0.25 µl internal size standard (500 ROX Size Standard, Applied Biosystems).
258 Labeled terminal-restriction fragments (T-RFs) were denatured at 95°C for 3 min, chilled on ice and
259 detected on an ABI 3130 automatic DNA sequencer (Applied Biosystems). Electropherograms were
260 compiled into numeric data using the Peak Scanner software (version 1.0, Applied Biosystems) and
261 fragment length with peak height >50 fluorescence units were used for profile comparison. Raw
262 data were normalized prior to statistical analysis (Dunbar et al., 2000).
263
264 2.4. Statistical data analysis
265 Data on abundance of the studied genes and soil chemical properties were subjected to ANOVA
266 using Statistical Analysis Software program (SAS V 9.2, SAS Institute Inc., North Carolina, USA).
267 For statistical analysis of the gene abundance data, a generalized linear mixed model with a
268 negative binomial distribution error and a log link function was used. Effects of straw addition
269 (factor "straw") and incubation time (factor "time") as well as the interaction between both factors
270 on abundance of all studied genes and on chemical properties were tested by two-way analysis of
271 variance (ANOVA). The data were checked for normality and homoscedasticity on model residuals
272 using quantile–quantile (Q–Q) plots, histograms and studentized residual plots.
273 Pearson linear correlation analyses were conducted and visualized for linearity in the SAS COR
274 procedure (data not shown) to relate the abundance of the target genes (dependent variables) to the
275 soil physico-chemical properties (independent variables).
276 Co-occurrence/co-exclusion analysis between the abundances of *arc-nosZ* and *gdh* genes and
277 chemical properties (NH_4^+, DON) was carried out by using the "corrplot" package of R
278 (http://www.r-project.org). The analysis was performed controlling the "False Discovery Rate"

279 (FDR), as described by Benjamini and Hochberg (1995). The adjustment methods include the
280 Bonferroni correction ("bonferroni") in which the p-values are multiplied by the number of
281 comparisons.
282 TRFLP data sets were analyzed using Bray-Curtis similarity coefficients (Bray and Curtis, 1957). A
283 similarity matrix was generated for 16S archaea, total prokaryotic *nosZ* (*nosZ*) and archaeal *nosZ*
284 (*arc-nosZ*) target genes This similarity matrix was used for one-way analysis of similarity
285 (ANOSIM) statistics (Clarke, 1993) to test if the composition of target communities was altered by
286 factors “straw” , “time” and by “straw x time” interaction. ANOSIM is based on rank similarities
287 between the sample matrix and produces a test statistic ‘R’ (Rees et al., 2005). A ‘global’ R was
288 first calculated in ANOSIM, which evaluated the overall effect of a factor in the data set. This step
289 was followed by a pair wise comparison, whereby the magnitude of R indicated the degree of
290 separation between two tested communities. An R score of 1 indicated a complete separation, while
291 0 indicated no separation (Rees et al., 2005).
292 Statistical analysis of T-RFLP profiles was performed with Primer V6.1.13 software (Primer E,
293 Plymouth, UK) according to Rasche et al. (2011).
294 Additionally, to test the influence of NH_4 on the structure of *nosZ* and *arc-nosZ* genes among straw
295 and no straw treatments over the incubation time, principal component analysis (PCA) was
296 performed using the “dudi.pca” function of in R-package ade4 (Thioulouse et al. 1997; Dray et al.
297 2007). Thus, to indicate a redundancy in the data, a correlation matrix was constructed, where the
298 presence or absence as well as relative height of T-RFs were used as distinct data, whereas NH_4^+
299 data were included in the analysis as ‘environmental’ variable. The data were grouped by straw and
300 no straw treatments over the incubation time. The graph of the PCA represents the differences
301 induced by NH_4^+ in the community structures of *nosZ* and *arc-nosZ* genes across the treatments at
302 each sampling time: 1, 5, 10, 20, 30, and 60 days, according to the axes `x' and `y', which represent
303 eigen vectors with the greater variance.
304

3. Results

3.1. Soil chemical properties

After submergence, soil pH showed a progressive increase from 5.8 to 7.0 ($p<0.01$) after 60 days of incubation for both treatments with or without straw. This was in line with our previous results confirming the onset of anaerobic conditions with a decrease in redox potential (Eh) from +293 mV to –180 and +110 mV over the first 30 days of incubation, in the presence or absence of straw, respectively (Cucu et al., 2014).

N_2O fluxes from soils receiving straw were negligible throughout the incubation period, while soils not receiving straw showed a peak in N_2O emissions on the first three days immediately after mineral N addition, followed by negligible emissions for the remaining incubation period (Fig.1).

Under submerged conditions, NH_4^+ was the main inorganic N form (Figure 2a). In the presence of straw, NH_4^+ decreased from 57 mg N kg^{-1} to 41 mg N kg^{-1} in the first 20 days and subsequently increased to values similar to the initial concentration by the end of the incubation (time × straw interaction, $p<0.001$). In contrast, in the absence of straw, NH_4^+ concentrations decreased steadily to 23 mg N kg^{-1} by day 60 ($p<0.001$).

Soils receiving straw showed NO_3^- concentrations below detection limit throughout the incubation period (Fig. 2b). In the absence of straw, NO_3^- present at the beginning of the incubation (5 mg N kg^{-1}) rapidly disappeared within the first 5 days, followed by an increase with time reaching 4 mg N kg^{-1} at day 30 and 3 mg N kg^{-1} at day 60 ($p<0.001$).

TDN concentrations in soils receiving straw increased from 66 to 76 mg N kg^{-1} with time ($p<0.001$; Fig. 2c), and DON, calculated as the difference between TDN and mineral N (i.e., NH_4^+-N + NO_3^--N), increased from 10 to 20 mg N kg^{-1} at day 60. On the other hand, in soils without straw addition, TDN decreased from 66 to 32 mg N kg^{-1} by 60 days (time × straw interaction, $p<0.001$) mainly due to a loss of inorganic N-forms, since DON only varied from 10 to 6 mg kg^{-1} over the same time period.

During the entire incubation, soils with straw showed higher DOC concentrations with respect to soils without straw ($p<0.01$), with initial concentrations of approximately 155 mg and 79 mg C kg^{-1}, respectively (Fig. 2d). In both treatments, DOC contents decreased rapidly within the first 5 days of the incubation and increased thereafter reaching highest values by day 60 (192 and 110 mg C kg^{-1} in straw and no straw treatments, respectively). Increase of DOC was more pronounced for soils receiving straw (time × straw interaction, $p<0.01$).

3.2. Microbial abundance

Abundance of bacterial 16S rRNA genes generally decreased with time, particularly for soils receiving straw (time × straw interaction; $p<0.001$), with values ranging between 1.0×10^{10} and 2.7×10^{10} copy numbers g^{-1} soil (Fig. S1a). Variations in archaeal 16S rRNA gene abundance with time generally followed a trend similar to that observed for bacterial 16S rRNA gene abundance (time × straw interaction; $p<0.001$), also exhibiting a higher gene copy number in soils without straw (8.5×10^{9}) with respect to those with straw (6.5×10^{9}9. However, soil samples receiving straw showed a more pronounced decrease in archaeal 16S rRNA gene copy numbers from day 5 onwards with respect to bacterial 16S rRNA genes. After 60 days of incubation, archaeal 16S rRNA gene abundance declined to 1.1×10^{9} and 5.5×10^{8} copy numbers g^{-1} soil for the no straw and straw treatments, respectively (Fig. S1b).

Abundance of *gdhA* genes ranged from 1.3×10^{9} to 2.0×10^{9} copy numbers g^{-1} soil in the straw treatment, and from 1.1×10^{9} to 1.8×10^{9} copy numbers g^{-1} soil in the no straw treatment (Fig. S2). In both treatments, *gdhA* gene abundance decreased during the first 5 days of incubation, but subsequently increased with time, generally showing higher values for soils receiving straw than those not receiving straw by the end of the incubation time (time × straw interaction; $p<0.001$).

Abundance of total prokaryotic *nosZ* clade I genes ranged from 2.3×10^{7} to 8.6×10^{7} copy numbers g^{-1} soil in the straw treatment and from 2.5×10^{7} to 6.2×10^{7} copy numbers g^{-1} soil in the no straw treatment (Fig. 3a), while the abundance of *arc-nosZ* genes ranged from 7×10^{6} to 6.3×10^{7} copy

356 numbers g^{-1} soil and from 1.7×10^7 to 6.4×10^7 copy numbers g^{-1} soil for the straw and no straw
357 treatments, respectively (Fig. 3b). For both genes, the abundance tended to decrease during the first
358 10 days of incubation, particularly for the *arc-nosZ* genes in the straw treatment (time × straw
359 interaction; $p<0.001$) and increased again during the later phase of incubation (between 20-60
360 days).
361 The relative abundance of *arc-nosZ* genes with respect to total prokaryotic *nosZ* clade I genes,
362 expressed as *arc-nosZ*/*nosZ* ratio, varied during the incubation time from 0.6 to 1 and from 1 to 0.2
363 in the no straw and straw treatments, respectively (data not shown).
364 Soils not receiving straw showed stronger positive correlations between gene abundance and
365 chemical properties with correlation coefficients ranging from r = 0.216 ($p<0.01$) to 0.879
366 ($p<0.001$) (Table 3). On the other hand, soils receiving straw showed correlation coefficients
367 ranging between r = 0.153 ($p<0.01$) and 0.574 ($p<0.001$).
368 The co-occurrence and co-exclusion between *arc-nosZ* and *gdhA* gene abundance and NH_4^+ and
369 DON were investigated by considering the significant correlations at False Discovery Rate (FDR) <
370 0.05 (Fig. S3). Abundance of *arc-nosZ* genes showed positive correlations with the abundance of
371 the *gdhA* gene and NH_4^+ content, while a negative correlation was found for DON contents (FDR <
372 0.05).
373
374 3.3. Microbial community structure
375 ANOSIM was used to compare effects of "straw" and "time" on the community structure of
376 archaeal 16S rRNA gene, *nosZ* clade I genes and *arc-nosZ* genes (Table 4). Factor "time" had a
377 greater influence than factor "straw" on all studied genes ($p<0.001$). ANOSIM detected significant
378 interactions between both factors (archaeal 16S rRNA (R=0.724), total prokaryotic *nosZ* clade I
379 (R=0.691), *arc-nosZ* (R=0.735) genes; $p<0.001$)).
380 NH_4^+ had a distinct effect on the determined shifts in the community structures of *nosZ* and *arc-*
381 *nosZ* genes across the treatments during the incubation time (Fig. 4 and 5).The PCA clearly showed

382 a clustering of *nosZ* straw treated samples (Fig. 4a) from 10, 20 and 30 days which were well
383 separated from samples belonging to 1 and 5 and 60 days. A different pattern was revealed by the
384 PCA of *nosZ* no straw treated samples (Fig. 4b) which clustered in two different groups: samples
385 from 1 and 5 days and samples belonging to 10, 20, 30 and 60 days.
386 The PCA of *arc-nosZ* straw samples (Fig. 5a) showed a separation of samples from 10, 20, 30 and
387 60 days from samples belonging to 1 and 5 days, while the PCA of *arc-nosZ* no straw samples (Fig.
388 5b) revealed community differences between samples from 20, 30 and 60 days, separated from
389 samples belonging to 1, 5 and 10 days.
390
391 3.4. DNA ^{15}N-enrichment
392 Addition of labeled (99 atom% ^{15}N) $(NH_4)_2SO_4$ resulted in a progressive ^{15}N-enrichment of DNA
393 with respect to natural ^{15}N abundance (0.3663 atom% ^{15}N) (Fig. S4). The highest enrichment was
394 obtained after 30 days of incubation, corresponding to 6.8 and 5.4 atom% ^{15}N excess in the straw
395 and no straw treatments, respectively (time × straw interaction; $p<0.001$).
396
397 3.5. ^{15}N-SIP analysis
398 T-RFLP fingerprints of *arc-nosZ* genes were generated from heaviest SIP gradient fractions (1.70 to
399 1.76 g ml^{-1}) to identify those community members which most efficiently incorporated the ^{15}N
400 tracer (Fig. 6). As expected, community structure in fractions showed a lower diversity as compared
401 to the bulk samples, since only a part of the community was active in ^{15}N assimilation. In all
402 fractions, with or without straw, the *arc-nosZ* gene community was dominated by two T-RFs (i.e.,
403 191 and 273 bp), but also by other T-RFs (e.g., 107, 117, 164, 185 bp) which were detected in
404 several fractions. T-RFLP fingerprinting revealed a clear distinction in T-RF allocation between ^{14}N
405 (Fig. 6a and 6c) and ^{15}N SIP gradients (Fig. 6b and 6d) suggesting a successful ^{15}N enrichment in
406 the heaviest fractions.

Conversely, total *nosZ* gene clade I T-RFLP fingerprinting analysis showed no ^{15}N-enrichment in all fractions of both the straw and no straw treatments (data not shown).

Incorporation of the ^{15}N tracer in *arc-nosZ* genes was further corroborated by quantification of archaeal *gdhA* genes performed on heavy CsCl gradient fractions in both treatments, with or without straw. In the straw treatment (Fig. 7a), label incorporation was evident in the ^{15}N labeled gradient, where the gene abundance peak shifted to a buoyant density (BD) of 1.7594 g ml^{-1} compared to that of the ^{14}N control (1.7570 g ml^{-1}). This was similar in the no straw treatment, where the gene abundance peak in the ^{15}N gradient shifted to a BD of 1.7157 g ml^{-1} compared to the ^{14}N control with 1.6987 g ml^{-1} (Fig. 7b). The shift in BD of approximately 0.02 g ml^{-1} corresponded to 50% of the density shift of 0.04 g ml^{-1} expected for 100% label incorporation (Lueders et al., 2004). In addition, the presence of ^{15}N labeled DNA into even heavier fractions (BD of 1.7365 to 1.7560 g ml^{-1}) indicated an overall higher label incorporation in the no straw with respect to straw ^{15}N-gradient.

4. Discussion

4.1. Archaeal N assimilation

Rice straw addition to submerged rice paddy soils represented the key factor for observed diverse responses of total bacterial and archaeal communities. This suggested that soil N immobilization and gaseous losses – as quantified in the previous experiment as a function of straw application (Cucu et al., 2014) – were controlled by both bacteria and archaea. However, under our experimental conditions, the archaeal community showed a clear domination over bacteria, especially in the absence of straw. In contrast to denitrifying bacteria, which usually use a dissimilatory metabolism under non-limiting NH_4^+ conditions, archaeal denitrifiers rely on an assimilatory pathway to acquire N for formation of nucleic and amino acids as well as proteins (Cabello et al., 2004; Nannipieri and Paul, 2009; Rusch, 2013). This was confirmed by the high abundance of *gdhA* gene and progressive ^{15}N-enrichment of DNA that displayed the effective biotic

433 immobilization of N during incubation. These observations suggested that independently of straw
434 addition, archaeal N assimilation was an important process in the studied soil. Moreover, the similar
435 increase in *gdhA* gene abundance in both straw-treated and non-treated soils suggested that archaeal
436 assimilation under non-NH_4^+ limiting environments was hardly influenced by the presence of labile
437 organic C. However, the negative correlation between *gdhA* gene abundance and DOC indicated a
438 stronger influence of soil derived C sources with respect to that of added straw. Moreover, although
439 *gdhA* gene abundance was positively correlated with NH_4^+ content in both treatments, this
440 relationship was stronger for soils not receiving straw with respect to straw treated soils. On the
441 other hand, the stronger correlation between *gdhA* gene abundance and TDN (i.e., the sum of
442 inorganic and organic N) with respect to NH_4^+ for soils receiving straw suggested that, although
443 archaeal N assimilation was driven by NH_4^+ availability, archaea could have modified their
444 metabolism with time to obtain N from other easily accessible sources (e.g., dissolved organic N
445 (DON) from labile OM) (Offre et al., 2013). Support for this was given by the negative correlation
446 between *gdhA* gene abundance and DON which was in line with a rapid consumption and turnover
447 of this labile N pool and the consequent increase in inorganic available N forms (Cucu et al., 2014).
448 In addition, the slightly higher *gdhA* gene abundance in the presence of labile organic matter (OM)
449 could be most likely attributed to an enhanced supply of NH_4^+ resulting from the mineralization of
450 added straw and dissolved OM released under anoxic conditions (Cucu et al., 2014).
451
452 *4.2. N assimilation as support for archaeal denitrification*
453 ^{15}N-DNA-based SIP revealed specific archaeal community members involved in both N
454 assimilation and denitrification processes. The ^{15}N-labeled NH_4^+ was actively assimilated via *gdhA*
455 gene for subsequent utilization (e.g., N_2O reductase synthesis), N immobilization and community
456 growth. Although labeling success of DNA was apparently low in comparison to other studies (e.g.,
457 Buckley et al., 2007a; España et al., 2011), a clear labeling effect was observed in *arc-nosZ* gene
458 community fingerprints of 'heavy' fractions in ^{15}N-enriched samples compared to control

459 treatments. Moreover, NH_4^+ assimilation was confirmed by a higher abundance of *gdhA* gene in
460 heavy ^{15}N labeled fractions, especially in the absence of straw.
461 Total prokaryotic *nosZ* clade I gene fingerprinting in the SIP fractions showed no evident ^{15}N
462 assimilation (data not shown). This result indicated especially in the straw treatment the shift in the
463 total prokaryotic *nosZ* community towards bacterial members and suggested that bacterial
464 denitrifiers were most probably using only N as an electron sink and for energy conservation
465 (Zumft 1997). Archaeal N assimilation resulted in an increase in the abundance of assayed N_2O
466 reduction genes (*arc-nosZ*), indicating the predominance of denitrifying archaea compared to their
467 bacterial counterparts, especially in soils not receiving straw. This was confirmed by the high
468 relative abundance of *arc-nosZ* with respect to total prokaryotic *nosZ* clade I genes, as evidenced by
469 *arc-nosZ*/*nosZ* ratios. Since the abundance of total prokaryotic *nosZ* clade II genes is in the same
470 range of clade I (Jones et al., 2013), quantification of clade II may result in an underestimation of
471 the archaeal proportion of the total N_2O reducing community. However, archaeal members may still
472 have a significant role in completing the denitrification process. The abundance of total prokaryotic
473 *nosZ* clade I and specifically *arc-nosZ* genes was reflected in negligible N_2O emission fluxes over
474 the whole incubation period in both treatments. This confirmed that the gaseous losses of applied N
475 (up to 60%) in the absence of straw (c.f. only 20% lost in the presence of straw), reported by Cucu
476 et al (2014) could be mainly attributed to N_2 emissions. These findings were in line with previous
477 studies reporting high N_2O reduction under continuous rice soil flooding (DeDatta 1995; Ussiri and
478 Lal, 2013; Peyron et al., 2016).
479
480 *4.3. Resource driven archaeal NH_4^+ assimilation and denitrification*
481 It is generally assumed that net ammonification and consequently N availability are greater under
482 anaerobic soil conditions due to low metabolic N requirements of anaerobic microorganisms
483 (Reddy and DeLaune, 2008). However, our findings indicated that archaeal denitrifiers were able to

484 assimilate N under non-limiting NH_4^+ conditions and that this metabolic modification was most
485 likely a function of C and N availability.
486 Observed alterations of *arc-nosZ* gene community dynamics in soils without straw suggested a
487 greater efficiency in NH_4^+ assimilation and N immobilization than in the presence of straw. This
488 was probably due to a more competitive and versatile metabolism of chemoautotrophic
489 microorganisms (e.g., archaea) being well-adapted to resource limitation. Although it is generally
490 accepted that increased C substrate availability increases microbial population size (Anderson and
491 Domsch 1978; Fontaine et al, 2003) and thus activity, our results clearly indicated that under C
492 limiting conditions archaeal denitrifiers were most likely equipped with a unique metabolic
493 flexibility to scavenge alternative nutrient sources (Műller et al., 2014). Accordingly, in the absence
494 of alternative labile organic C (e.g., rice straw), the microbial communities might utilized carbon
495 dioxide as their main C source (Bock et al., 1991), reduced compounds (e.g., ammonium, iron(II),
496 and sulfide) as electron donors (Liesack et al., 2000; Megonigal et al., 2004), or N_2O as sole
497 electron acceptor (Stres et al., 2004; Strohm et al., 2007; Braker and Conrad, 2011). This suggested
498 a contrast with the general assumption that prokaryotic denitrifiers are predominantly heterotrophic
499 (Parkin 1987).
500 Independent of the adopted agricultural management, our results might display that rice paddy soils
501 act as temporary sink for N_2O. Furthermore, abundance of both denitrifying genes was positively
502 correlated to NH_4^+ and TDN concentrations highlighting the co-occurence of both complete
503 denitrification and ammonification in the same genome (Tiedje et al., 1988; Sanford et al., 2012).
504 Support for this was also given through the negative correlation of *arc-nosZ* gene abundance with
505 DON contents. Likewise, mineralization promotes the recycling of immobilized N which may then
506 enter further processes including denitrification (Nannipieri et al., 2003).
507 As expected, the higher availability of labile C with straw addition under non-limiting N conditions
508 induced N assimilation but also a lower abundance of total *nosZ* clade I and *arc-nosZ* genes, as well
509 as distinct variation in the community structure of these genes. Lower abundance of *nosZ* genes in

510 the presence of straw was in contrast with other studies (Chen et al., 2012a,b). However, at the later
511 stages of incubation, when most of added straw was probably decomposed, progressively higher
512 abundance of *nosZ* and *arc-nosZ* genes was positively related to DOC content which was in line
513 with the findings of Kandeler et al., (2006) and Philippot et al., (2009). Labile organic C served as
514 resource for denitrifying bacteria that outcompeted archaeal counterparts, as evidenced by a
515 decreasing *arc-nosZ/nosZ* ratio with incubation time. This was in agreement with Ishii et al.
516 (2011b) who, by using functional single-cell (FSC) and DNA-based SIP with ^{13}C-labeled succinate
517 as electron donor and N_2O as electron acceptor showed that under their experimental conditions,
518 most N_2O reducers are bacterial denitrifiers. Examining the N_2O reduction rates of the isolated
519 strains, the authors confirmed the growth of putative bacterial denitrifiers reciprocally to N_2O
520 reduction in rice field soils, although many bacteria have only partial pathways of denitrification
521 (Shapleigh, 2013).
522
523 **5. Conclusions and outlook**
524 Nitrogen immobilization based on archaeal NH_4^+ assimilation was shown to represent an important
525 step for proliferation and dynamics of those microbial community members harboring the *arc-nosZ*
526 gene encoding N_2O reductase enzyme, irrespective of the presence or absence of labile OM. Under
527 our experimental conditions, the relative abundance of *arc-nosZ* genes with respect to total
528 prokaryotic *nosZ* from clade I genes was based on an adaptable metabolic portfolio. However, in
529 the presence of straw, bacterial *nosZ* genes may also contribute to the completion of denitrification.
530 Based on these considerations, we developed a conceptual model to represent the archaeal N
531 assimilation and denitrification pathways driven by different resources under anaerobic conditions
532 (Fig. 8). The response of *arc-nosZ* genes to different C availability under non-limiting N conditions
533 may have important ecological implications in controlling the immobilization and loss of N from
534 fertilized paddy soils. Furthermore, the high adaptability of archaea to drive denitrification to
535 completion may be a key feature in mitigating N_2O emissions.

536 The present study suggested the potential contribution of archaea to the last step of denitrification
537 when favorable environmental conditions are given as complement to the bacterial counterparts
538 from *nosZ* clade I. However, although we have provided important insights, the full understanding
539 of archaeal involvement in the denitrification process remains still incomplete. This accounts
540 particularly for the currently limited phylogenetic information on *arc-nosZ* gene synthesizing
541 archaea in soils (Rusch 2013). Hence, we strongly suggest the generation of *arc-nosZ* gene libraries
542 to enhance phylogenetic knowledge on this particular gene. In addition, prospective research should
543 also consider the unconsidered *nosZ* gene (e.g., clade II, atypical *nosZ*) to better understand the
544 relative role of archaea in acting as N_2O sink.
545 As N assimilation processes are regulated by resource availability, we recommend evaluating the
546 effects of different N fertilizer and organic residue types with contrasting C/N ratio. In this respect,
547 ^{15}N and ^{13}C-label SIP-based studies may be appropriate to evaluate the metabolic adaptability of
548 archaea for mineral and organic substrate consumption and their implication in mitigating emissions
549 of climate relevant gases from paddy soils.
550

551 **Funding**
552 This work was partly supported by the Italian Ministry of Agriculture, Food and Forestry
553 (MiPAAF) under the project "Sustaining the National Rice Industry through Research, Technology,
554 Innovation and Formation (POLORISO)" and International Humic Substance Society (IHSS).
555

556 A**cknowledgements**
557 We gratefully thank R. Gorra (Department of Agricultural, Forest and Food Sciences, University of
558 Turin, Italy) for fruitful discussions; J. Laso (Department of Bioinformatics, University of
559 Hohenheim, Germany) and I. Ferrocino (Department of Agricultural, Forest and Food Sciences,
560 University of Turin, Italy) for their support in statistical analysis. The authors are further grateful to
561 L. Hölzle (Institute of Animal Science, University of Hohenheim) for access to his ABI 3130

562 Genetic Analyzer and C. Röhl (Institute of Plant Production and Agroecology in the Tropics and
563 Subtropics, University of Hohenheim) for her technical support.

564 **References**

565 Anderson JPE, Domsch KH (1978) A physiological method for the quantitative measurement of
566 microbial biomass in soils. Soil Biol Biochem: 10: 215–221

567 Bird JA, Horwáth WR, Eagle AJ, van Kessel (2001) Immobilization of fertilizer nitrogen in rice.
568 Soil Sci Soc Am J 65:1143-1152

569 Benjamini Y, Hochberg Y (1995) Controlling the false discovery rate: a practical and powerful
570 approach to multiple testing. J R Stat Soc Series B 57: 289–300

571 Bray JR, Curtis JT (1957) An ordination of the upland forest communities of southern Wisconsin.
572 Ecol Monogr 27:325-349

573 Bock E, Koops HP, Harms H, Ahlers B (1991) The biochemistry of nitrifying organisms. In:
574 Shively JM, Barton LL (eds) Variations in autotrophic life, London, Academic Press, pp
575 171-200

576 Bonete MJ, Martínez-Espinosa RM, Pire C, Zafrilla B, Richardson DJ (2008) Nitrogen metabolism
577 in haloarchaea. Saline Systems 4:9

578 Braker G and Conrad R. Diversity, structure, and size of N_2O-producing microbial communities in
579 soils–what matters for their functioning? (2011) In: Laskin I, Sariaslani S, Gadd GM (eds)
580 Advances in Applied Microbiology, vol.75, SanDiego, Elsevier Academic Press Inc., pp 33–
581 70

582 Buckley DH, Huangyutitham V, Hsu SF, Nelson TA (2007a) Stable isotope probing with $^{15}N_2$
583 reveals novel non-cultivated diazotrophs in soil. Apppl Environ Microbiol 73:3196-3204

584 Buckley DH, Huangyutitham V, Hsu SF, Nelson TA (2007b) Stable isotope probing with ^{15}N
585 achieved by disentangling the effects of genome G+C content and isotope enrichment on
586 DNA density. Appl Environ Microbiol 73:3189-3195

587 Cabello P, Roldán MD, Moreno-Vivían C (2004) Nitrate reduction and the nitrogen cycle in
588 archaea. Microbiol 150:3527-3546

589 Cassman KG, Peng S, Olk DC, Ladha JK, Reichardt W, Dobermann A, Singh U (1998)
590 Opportunities for increased nitrogen-use efficiency from improved resource management in
591 irrigated rice systems. Field Crop Res 56:7-39
592 Cassman KG, Dobermann A, Walters DT (2002) Agro-ecosystems, nitrogen-use efficiency, and
593 nitrogen management. Ambio 31:132-140
594 Chen Z, Liu J, Wu M, Xie X, Wu J, Wei W (2012a) Differentiated response of denitrifying
595 communities to fertilization regime in paddy soil. Microb Ecol 63:446-459
596 Chen Z, Hou H, Zheng Y, Qin H, Zhu Y, Wu J, Wei W (2012b) Influence of fertilization regimes
597 on a *nosZ*-containing denitrifying community in a rice paddy soil. J Sci Food Agr 92:1064-
598 1072
599 Chuang H-P, Wu J-H, Ohashi A, Abe K, Hatamato M (2014) Potential of nitrous oxide conversion
600 in batch and down-flow hanging sponge bioreactor systems. Sustain Environ Res 24:117-
601 128
602 Clarke KR (1993) Non-parametric multivariate analyses of changes in community structure. Aust J
603 Ecol 18: 117-143
604 Conrad R (1995) Soil microbial processes involved in production and consumption of atmospheric
605 trace gasses. In: Jones JG (ed) Advances in Applied Microbiology, New York. Plenum
606 Press, pp 207-250
607 Conrad R (1996) Soil microorganisms as controllers of atmospheric trace gases (H_2, CO, CH_4,
608 OCS, N_2O, and NO). Microbiol Rev 60:609-640
609 Cucu MA, Said-Pullicino D, Maurino V, Bonifacio E, Romani M, Celi L (2014) Influence of redox
610 conditions and rice straw in corporation on nitrogen availability in fertilized paddy soils.
611 Biol Fertil Soil 50:755-764
612 Davidson EA, Swank WT, Perry TO (1986) Distinguishing between nitrification and denitrification
613 as sources of gaseous nitrogen production in soil. Appl Environ Microb 52:1280-1286
614 DeDatta SK (1995) Nitrogen transformations in wetland rice ecosystem. Fert Res 42:193-203

615 de Vries S, Schröder I (2002) Comparison between the nitric oxide reductase family and its aerobic
616 relatives, the cytochrome oxidases. Biochem SocTrans 30:662-667
617 Devêvre OC, Horwáth WR (2001) Stabilization of fertilizer nitrogen-15 into humic substances in
618 aerobic vs. waterlogged soil following straw incorporation. Soil Sci Soc Am J 65:499-510
619 Dray S, AB Dufour (2007) The ade4 package implementing the duality diagram for ecologist. J Stat
620 Softw 22:1-20
621 Dunbar J, Ticknor LO, Kuske CR (2000) Assessment of microbial diversity in four south western
622 United States soils by 16S rRNA gene terminal restriction fragment analysis. Appl Environ
623 Microb 66:2943-2950
624 Eagle AJ, Bird JA, Horwáth WR, Linquist BA, Brouder SM et al (2000) Rice yield and nitrogen
625 utilization efficiency under alternative straw management practices. Agronom J 92:1096-
626 1103
627 España M, Rasche F, Kandeler E, Brune T, Rodriguez B et al (2011) Identification of active
628 bacteria involved in decomposition of complex maize and soybean residues in a tropical
629 Vertisol using ^{15}N-DNA stable isotope probing. Pedobiologia 54:187-193
630 Fazli P, Hasfalina CM, UmiKalsom MS, Azni I (2013) Review Article: Characteristics of
631 methanogens and methanotrophs in rice fields. AsPac J Mol Biol Biotechnol 21: 3-17
632 Ferrè C, Zechmeister-Boltenstern S, Comolli R, Andersson M, Seufert G (2012) Soil microbial
633 community structure in a rice paddy field and its relationships to CH_4 and N_2O fluxes. Nutr
634 Cycl Agrosyst 93:35-50
635 Fetzer S, Bak F, Conrad R (1993) Sensitivity of methanogenic bacteria from paddy soil to oxygen
636 and desiccation. FEMS Microbiol Ecol 12:107–115
637 Fontaine S, Mariotti A, Abbadie L (2003) The priming effect of organic matter: a question of
638 microbial competition? Soil Biol Biochem 35:837-843

639 Garcia JL, Tiedje JM (1982) Denitrification in rice soils. In: Dommergues YR, Diem HG (eds)
640 Microbiology of tropical soils and plant productivity. Springer Netherlands, Dordrecht, pp
641 187-208.
642 Ghosh BC, Bhat R (1998) Environmental hazards of nitrogen loading in wetland rice fields.
643 Environ Pollut 102:123-126
644 Henry S, Bru D, Stres B, Hallet S, Philippot L (2006) Quantitative detection of the *nosZ* gene,
645 encoding nitrous oxide reductase, and comparison of the abundances of 16S rRNA, *narG*,
646 *nirK*, and *nosZ* genes in soils. Appl Environ Microbiol 72:5181-5189
647 Hutchinson GL, Mosier AR (1981) Improved soil cover method for field measurement of nitrous
648 oxide fluxes. Soil Sci Soc Am J, 45: 311–316
649 Ishii S, Ikeda S, Minamisawa K, Senoo K (2011a) Nitrogen cycling in rice paddy environments:
650 past achievements and future challenges. Microbes Environ J 26:282-292
651 Ishii S, Ohno H, Tsuboi M, Otsuka S, Senno K (2011b) Identification and isolation of active N_2O
652 reducers in rice paddy soil. ISME J 5:1936-1945
653 Jones CM, Graf DRH, Bru D, Philippot L, Hallin S (2013) The unaccounted yet abundant nitrous
654 oxide-reducing microbial community: a potential nitrous oxide sink. ISME J 7:417-426
655 Kandeler E, Deiglmayr K, Tscherko D, Bru D, Philippot L (2006) Abundance of *narG*, *nirS*, *nirK*,
656 and *nosZ* genes of denitrifying bacteria during primary successions of a glacier foreland.
657 Appl Environ Microbiol 72:5957-5962
658 Kögel-Knabner I, Amelung W, Cao Z, Fiedler S, Frenzel P, Jahn R et al (2010) Biogeochemistry of
659 paddy soils. Geoderma 157:1-14
660 Lane D (1991) 16S/23S rRNA sequencing. In: Stackebrandt A and Goodfellow M (eds) Nucleic
661 Acid Techniques Systematics, UK, John Wiley, West Sussex, pp 115–175
662 Liesack W, Schnell S, Revsbech NP (2000) Microbiology of flooded rice paddies. FEMS Microbiol
663 Rev 24:625-645

664 Lueders T, Friedrich M (2000) Archaeal population dynamics during sequential reduction processes
665 in rice field soil. Appl Environ Microbiol 66:2732-2742
666 Lueders T, Manefield M, Friedrich MW (2004) Enhanced sensitivity of DNA and rRNA based
667 stable isotope probing by fractionation and quantitative analysis of isopycnic centrifugation
668 gradients. Environ Microbiol 6:73-78
669 Majumdar D (2013) Biogeochemistry of N_2O uptake and consumption in submerged soils and rice
670 fields and implications in climate change. Crit Rev Env Sci Technol 43:2653-2684
671 Martİnez-Espinosa RM, Marhuenda-Egea FC, Bonete MJ (2001) Assimilatory nitrate reductase
672 from the haloarchaeon *Haloferax mediterranei*: purification and characterization. FEMS
673 Microbiol Lett 204:381–385
674 Megonigal JP, Hines ME, Visscher PT (2004) Anaerobic metabolism: linkages to trace gases and
675 aerobic processes. In: Schlesinger WH (ed) Biogeochemistry, Oxford, UK, Elsevier-
676 Pergamon, pp 317-424
677 Mulec MI, Ausec L, Danevčič T, Levičnik-Höfferle Š, Jerman V, Kraigher B (2014) Microbial
678 community structure and function in peat soil. Food Technol Biotechnol 52:180-187
679 Műller J, Hense BA, Marozava S, Kuttler Ch, Meckenstock RU (2014) Model selection for
680 microbial nutrient uptake using a cost-benefit approach. Math Biosci 255:52-70
681 Muyzer G, Dewaal EC, Uitterlinden AG (1993) Profiling of complex microbial populations by
682 denaturing gradient gel electrophoresis analysis of polymerase chain reaction-amplified
683 genes coding for 16S rRNA. Appl Environ Microbiol 59:695-700
684 Nannipieri P, Ascher J, Ceccherini MT, Landi L, Pietramellara G, Renella G (2003) Microbial
685 diversity and soil functions. Europ J Soil Sc 54:655-670
686 Nannipieri P, Paul EA (2009) The chemical and functional characterization of soil N and its biotic
687 components. Soil Biol Biochem 41:2357-2369
688 Neufeld JD, Vohra J, Dumont MG, Lueders T, Manefield M et al (2007) DNA stable-isotope
689 probing. Nat Protoc 2:860-866

690 Nogales B, Timmis KN, Nedwell DB, Osborn AM (2002) Detection and diversity of expressed
691 denitrification genes in estuarine sediments after reverse transcription-PCR amplification
692 from mRNA. Appl Environ Microbiol 68:5017-5025
693 Offre P, Spang A, Schleper C (2013) Archaea in biogeochemical cycles. Ann Rev Microbiol 67:
694 437-457
695 Parkin TB (1987) Soil microsites as a source of denitrification variability. Soil Sci Soc Am J 51:
696 1194-1199
697 Peyron M, Bertora C, Pelissetti S, Said-Pullicino D, Celi L, Miniotti E, Romani M, Sacco D (2016)
698 Greenhouse gas emissions as affected by different water management practices in temperate
699 rice paddies. Agric Ecosyst Environ 232:17-28
700 Philippot L (2002) Denitrifying genes in bacterial and archaeal genomes. Biochim Biophys Acta
701 1577:355-376
702 Philippot L, Čuhel J, Saby NPA, Chèneby D, Chroňáková A, Bru D et al (2009) Mapping field-
703 scale spatial distribution patterns of size and activity of the denitrifiers community. Environ
704 Microbiol 11:1518-1526
705 Prieme A, Braker G, Tiedje JM (2002) Diversity of nitrite reductase (*nirK* and *nirS*) gene fragments
706 in forested upland and wetland soils. Appl Environ Microbiol 68:1893-1900
707 Rasche F, Hödl V, Poll C, Kandeler E, Gerzabek MH, Van Elsas JD et al (2006) Rhizosphere
708 bacteria affected by transgenic potatoes with antibacterial activities compared with the
709 effects of soil, wild type potatoes, vegetation stage and pathogen exposure. FEMS Microbiol
710 Ecol 56: 219-235
711 Rasche F, Knapp D, Kaiser C, Koranda M, Kitzler B, Zechmeister-Boltenstern S et al (2011)
712 Seasonality and resource availability control bacterial and archaeal communities in soils of a
713 temperate beech forest. ISME J 5:389-402
714 Rees GN, Baldwin DS, Watson GO, Perryman,S, Nielsen DL (2005) Ordination and significance
715 testing of microbial community composition derived from terminal restriction fragment

length polymorphisms: application of multivariate statistics. Ant Van Leeuwenhoek 86: 339-347. http://dx.doi.org/10.1007/s10482-005-0498-5

Reddy KR (1982) Nitrogen cycling in a flooded-soil ecosystem planted to rice (*Oryza sativa* L.). Plant Soil J 67:209-220

Reddy KR, deLaune RD (2008) Biogeochemistry of wetlands: science and applications, USA, CRC Press, Boca Raton, FL

Rice CW, Tiedje JM (1989) Regulation of nitrate assimilation by ammonium in soils and in isolated soil microorganisms. Soil Biol Biochem 21:597-602

Rusch A (2013) Molecular tools for the detection of nitrogen cycling. Article ID 676450, Archaea doi:10.1155/2013/676450

Rusch A (2016) Archaea. In Kennish MJ (ed) Encyclopedia of Estuaries, Chapter: 287, Springer Science, Business Media Dordrecht, doi: 10.1007/978-94-017-8801-4_287, pp 35-37

Sahrawat KL (2004) Ammonium production in submerged soils and sediments: the role of reducible iron. Commun Soil Sci Plant Anall 35:399-411

Said-Pullicino D, Cucu MA, Sodano M, Birk JJ, Glaser B, Celi L (2014) Nitrogen immobilization in paddy soils as affected by redox conditions and rice straw incorporation. Geoderma 228-229:44-53

Samuel BS, Hansen EE, Manchester JK, Coutinho PM, Henrissat B, Fulton R et al (2007) Genomic and metabolic adaptations of *Methanobrevibacter smithii* to the human gut. PNAS J 104: 10643-10648

Sanford RA, Wagner DD, Wu Q, Chee-Sanford JC, Thomas SH, Cruz-Garcia C et al (2012) Unexpected nondenitrifier nitrous oxide reductase gene diversity and abundance in soils. PNAS J 48:19709-19714

Shapleigh JP. Denitrifying prokaryotes (2013). In: Rosenberg E et al (eds) Prokaryotes. Prokaryotic Physiology and Biochemistry, Berlin Heidelberg, Springer-Verlag, pp 405-425

741 Stres B, Mahne I, Avgustin G, Tiedje JM (2004) Nitrous oxide reductase (*nosZ*) gene fragments
742 differ between native and cultivated Michigan soils. Appl Environ Microbiol 70:301–309
743 Strohm TO, Griffin B, Zumft WG, Schink B (2007) Growth yields in bacterial denitrification and
744 nitrate ammonification. Appl Environ Microbiol 73:1420–1424
745 Thioulouse J, Chessel D, Doledec S, Olivier JM (1997) ADE-4: a multivariate analysis and
746 graphical display software. Stat Comput 7:75–83
747 Tiedje JM (1988) Ecology of denitrification and dissimilatory nitrate reduction to ammonium. In:
748 Zehnder AJB (ed) Biology of Anaerobic Microorganisms, New York, John Wiley & Sons,
749 pp 179-244
750 Tomlinson GA, Jahnke LL, Hochstein LI (1986) *Halobacterium denitrificans* sp. nov., an extremely
751 halophilic denitryfing bacterium. Int J Syst Bacteriol 36:66-70
752 Ussiri D, Lal R (2013) Nitrous oxide emissions from rice fields. In: Soil emission of nitrous oxide
753 and its mitigation, Netherlands, Springer, pp 213-242
754 WRB, IUSS Working Group WRB, 2007. World Reference Base for Soil Resources 2006, first
755 update 2007. World Soil Resources Reports No. 103. FAO, Rome, Italy
756 Zou J, Huang Y, Zheng X, Wang Y (2007) Quantifying direct N_2O emissions in paddy fields during
757 rice growing season in mainland China: dependence on water regime. Atm Environ 41**:**
758 8030-8042
759 Zumft WG (1992) The denitrifying prokaryotes. In: Balows A, Trüper HG, Dworkin M, Harder W,
760 Schleifer K-H (eds) The prokaryotes. A handbook on the biology of bacteria:
761 ecophysiology, isolation, identification, application, New York, Berlin, Heidelberg,
762 Springer-Verlag, 2nd edn, vol 1, pp 554-582
763 Zumft WG (1997) Cell biology and molecular basis of denitrification. Microbiol Mol Biol Rev 61:
764 533-616

766 **Figure Captions**
767

768 **Fig. 1** Daily nitrous oxide (N_2O) flux over time in soils incubated with or without straw addition.
769 The error bars (n=3) represent the least significant difference at p=0.05

770

771 **Fig. 2** Variations in concentrations of ammonium (sum of submergence water and soil extractable
772 NH_4^+) concentrations (a), nitrate (sum of submergence water and soil extractable NO_3^-) (b), total
773 dissolved N (sum of submergence water and soil water-extractable N) (c), and dissolved organic C
774 (sum of submergence water and soil water-extractable C) (d) with time for soils incubated with or
775 without straw addition. The error bars (n=6) represent the least significant difference at p=0.05

776

777 **Fig. 3** Abundance of total prokaryotic *nosZ* clade I (a) and *arc-nosZ* (b) genes over time in soils
778 incubated with or without straw addition (n=6, means with standard errors). Different letters above
779 bars indicate significant differences at $p<0.05$ between straw and no straw treatments at every
780 sampling time (lowercase letters) as well as significant differences among different sampling times
781 (uppercase letters).

782

783 **Fig. 4** Principal component analysis (PCA) of TRFLP profiles using *nosZ* gene T-RF relative
784 abundance data obtained form straw (a) and no straw (b) treatments in function of NH_4^+
785 concentration. Sampling time are indicated with colors (T 1 day – blue; T 5 days – red; T 10 days
786 – purple; T 20 days – pink; T 30 days – dark grey; T 60 days – green)

787

788 **Fig. 5** Principal component analysis (PCA) of TRFLP profiles using *arc- nosZ* gene T-RF relative
789 abundance data obtained form straw (a) and no straw (b) treatments in function of NH_4^+
790 concentration. Sampling time are indicated with colors (T 1 day – blue; T 5 days – red; T 10 days
791 – purple; T 20 days – pink; T 30 days – dark grey; T 60 days – green)

792

793 **Fig. 6** T-RFLP fingerprints of *arc-nosZ* genes generated from density resolved SIP fractions of the
794 straw ^{14}N-$(NH_4)_2SO_4$ (a), ^{15}N-$(NH_4)_2SO_4$ (b) and the no straw ^{14}N-$(NH_4)_2SO_4$ (c), and ^{15}N-
795 $(NH_4)_2SO_4$ (d) treatment. Buoyant densities (g ml^{-1}) of analyzed fractions are given in parentheses

796

797 **Fig. 7** Quantification of archaeal *gdhA* genes in comparative CsCl density fractions of DNA
798 extracted from straw (a) and non-straw (b) treatments fertilized with either ^{14}N- or ^{15}N-^{15}N-
799 $(NH_4)_2SO_4$

800

801 **Fig. 8** Schematic relationship between C and N resource availability and nitrogen assimilatory
802 archaeal denitrification in fertilized paddy soils suggesting the ecological importance of this
803 pathway

804

Graphical abstract

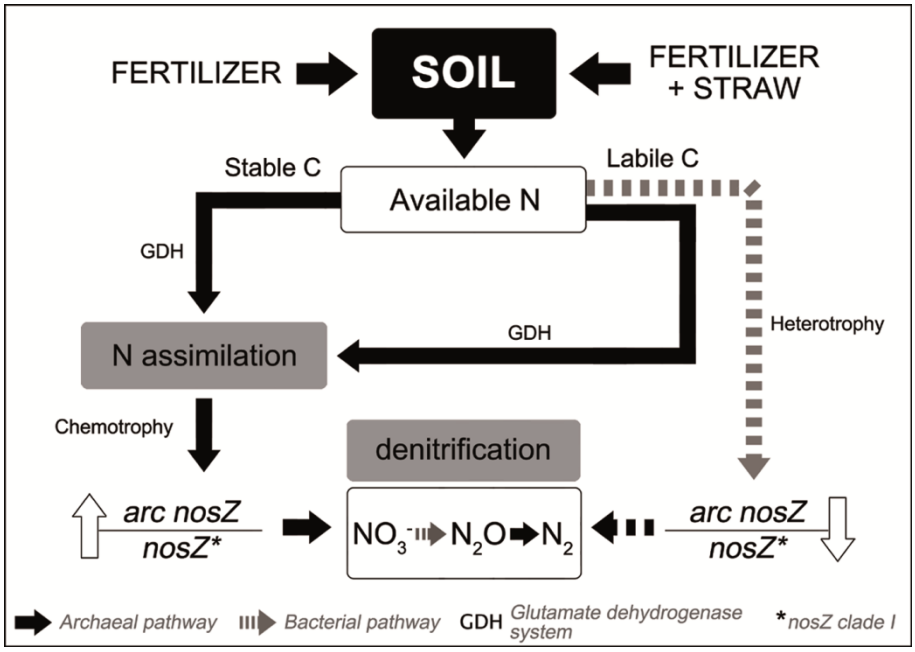

Figure 1

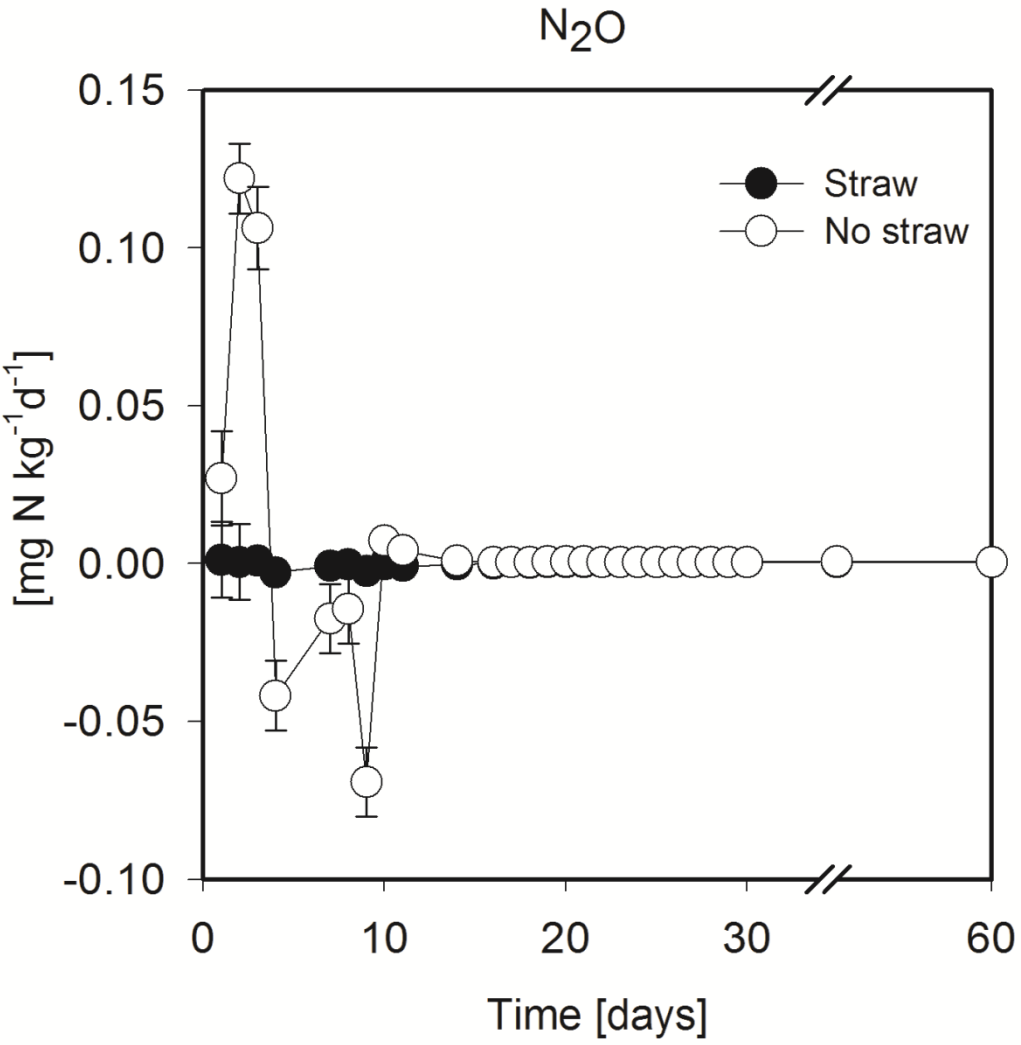
N2O
0.15
0.10
0.05
0.00
-0.05
-0.10
[mg N kg-1d-1]
Straw
No straw
0
10
20
30
60
Time [days]

Figure 2

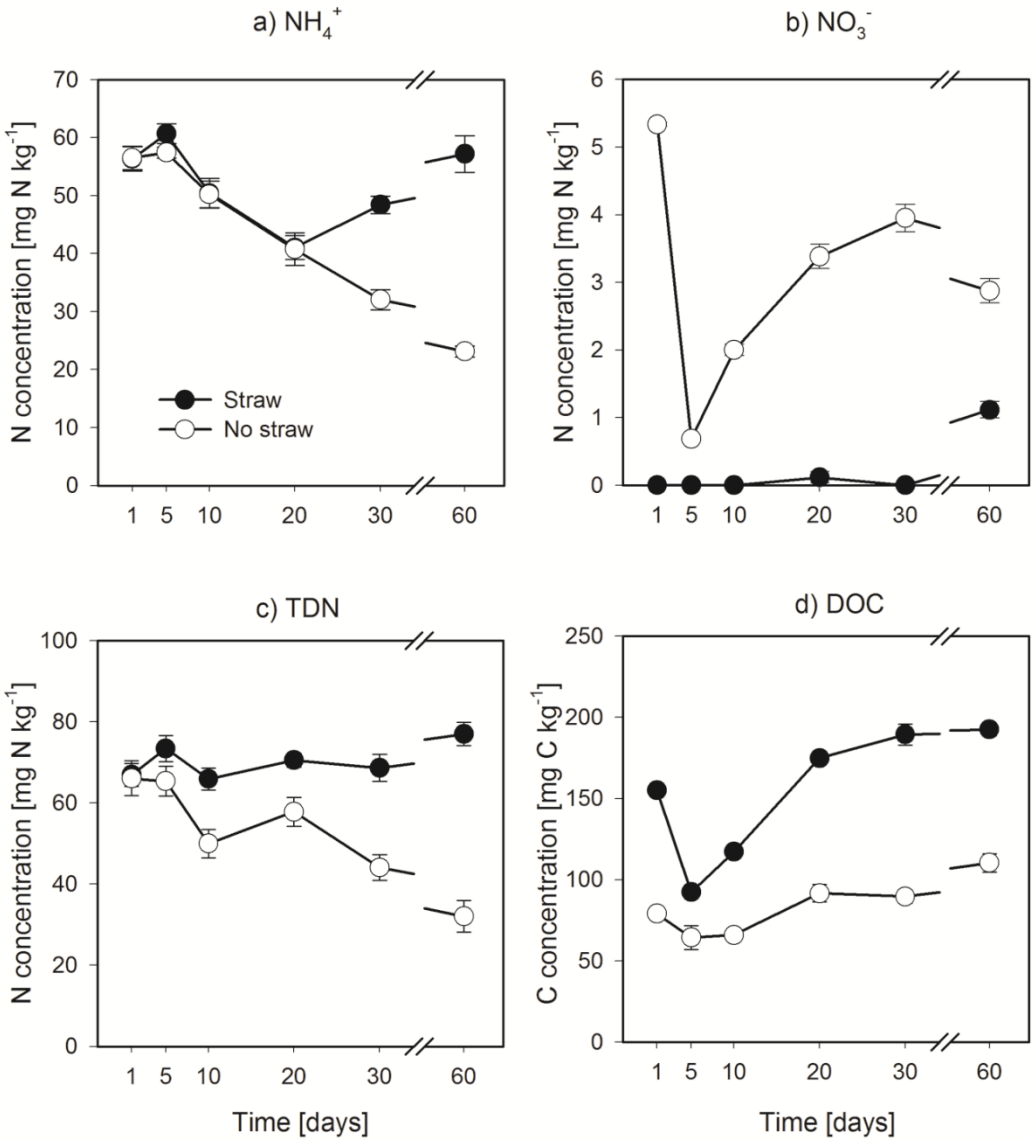
a) NH4+
b) NO3-
c) TDN
d) DOC
N concentration [mg N kg-1]
C concentration [mg C kg-1]
Straw
No straw
Time [days]
1 5 10 20 30 60
0 10 20 30 40 50 60 70
0 1 2 3 4 5 6
0 20 40 60 80 100
0 50 100 150 200 250

Figure 3

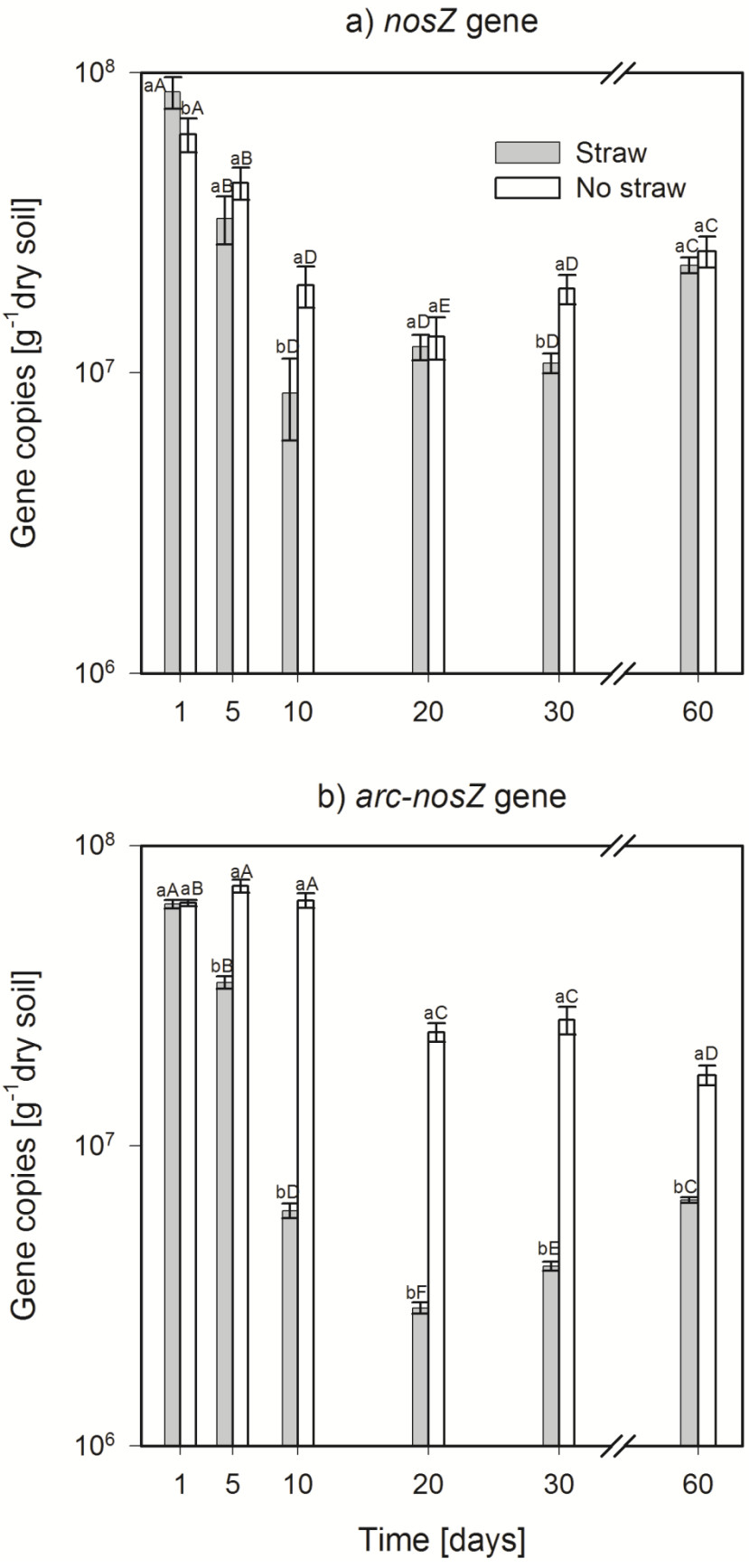
a) nosZ gene
Straw
No straw
Gene copies [g-1dry soil]
10^8
10^7
10^6
aA
bA
aB
aB
aD
bD
aE
aD
bD
aD
aC
aC
1
5
10
20
30
60
b) arc-nosZ gene
Gene copies [g-1dry soil]
10^8
10^7
10^6
aA aB
aA
aA
bB
bD
aC
bF
aC
bE
aD
bC
1
5
10
20
30
60
Time [days]

Figure 4

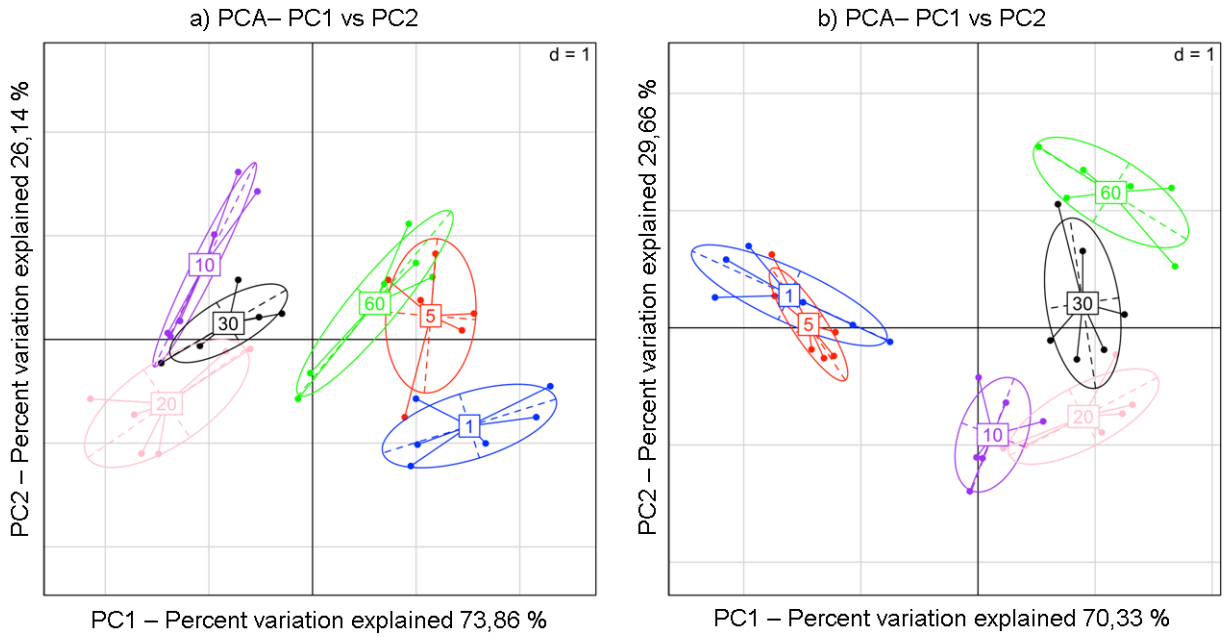
a) PCA– PC1 vs PC2
d = 1
PC2 – Percent variation explained 26,14 %
PC1 – Percent variation explained 73,86 %
10
30
20
60
5
1
b) PCA– PC1 vs PC2
d = 1
PC2 – Percent variation explained 29,66 %
PC1 – Percent variation explained 70,33 %
60
30
1
5
10
20

Figure 5

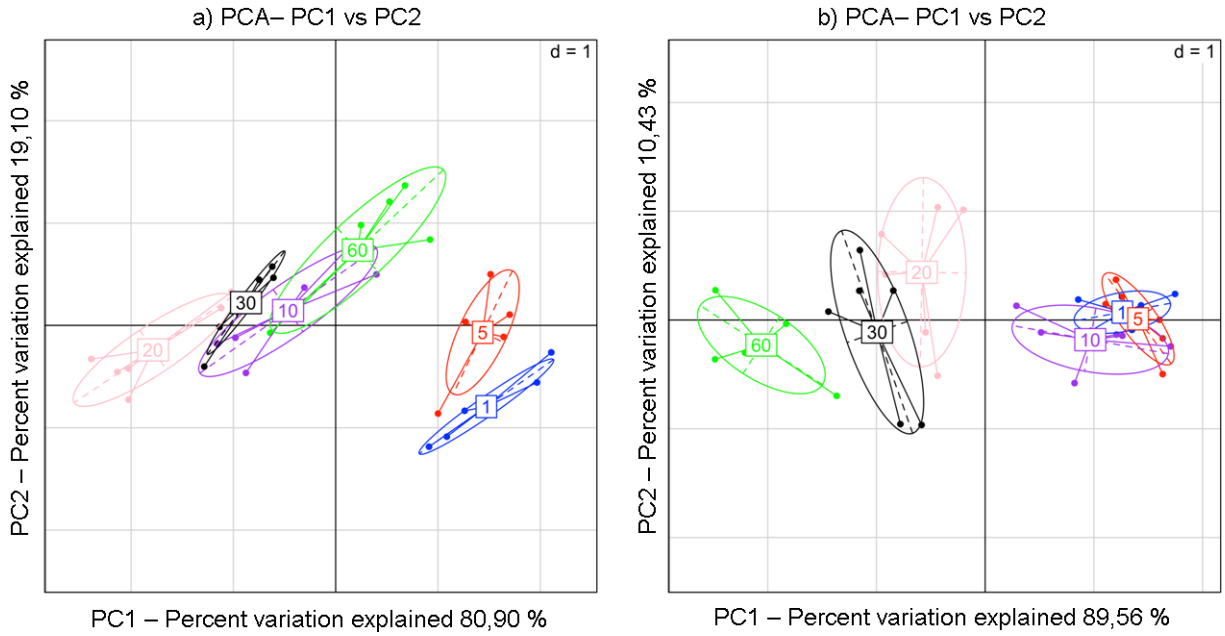
a) PCA– PC1 vs PC2
d = 1
PC2 – Percent variation explained 19,10 %
PC1 – Percent variation explained 80,90 %
20
30
10
60
5
1
b) PCA– PC1 vs PC2
d = 1
PC2 – Percent variation explained 10,43 %
PC1 – Percent variation explained 89,56 %
20
60
30
1
5
10

Figure 6

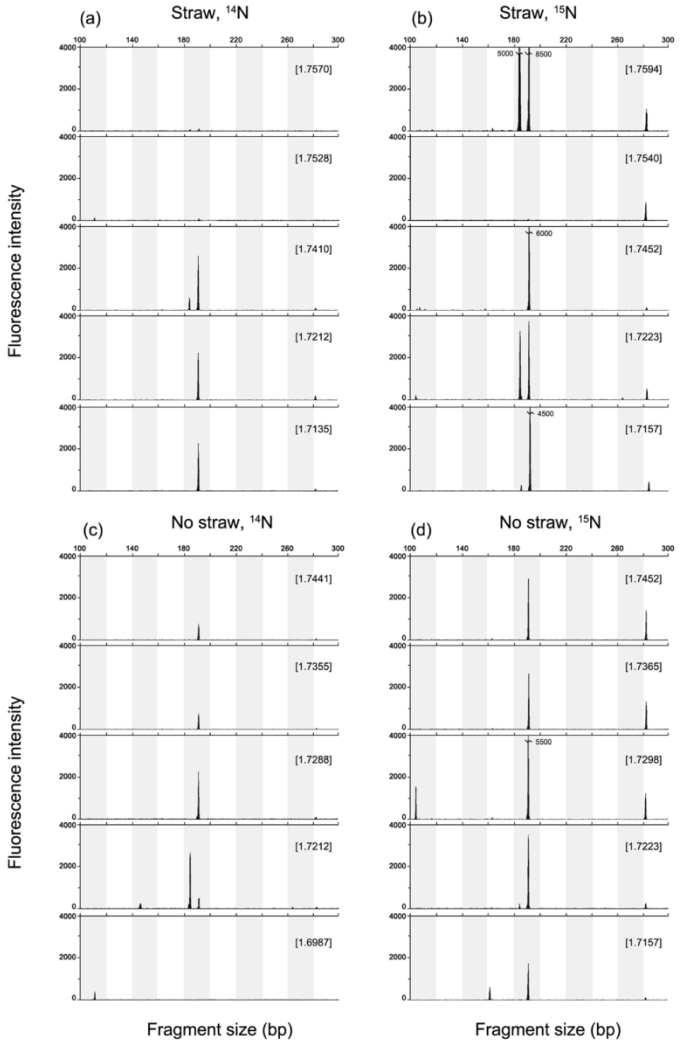
(a)
Straw, 14N
(b)
Straw, 15N
(c)
No straw, 14N
(d)
No straw, 15N
Fluorescence intensity
Fragment size (bp)
[1.7570]
[1.7528]
[1.7410]
[1.7212]
[1.7135]
[1.7594]
[1.7540]
[1.7452]
[1.7223]
[1.7157]
[1.7441]
[1.7355]
[1.7288]
[1.7212]
[1.6987]
[1.7452]
[1.7365]
[1.7298]
[1.7223]
[1.7157]
5000
8500
6000
4500
5500

Figure 7

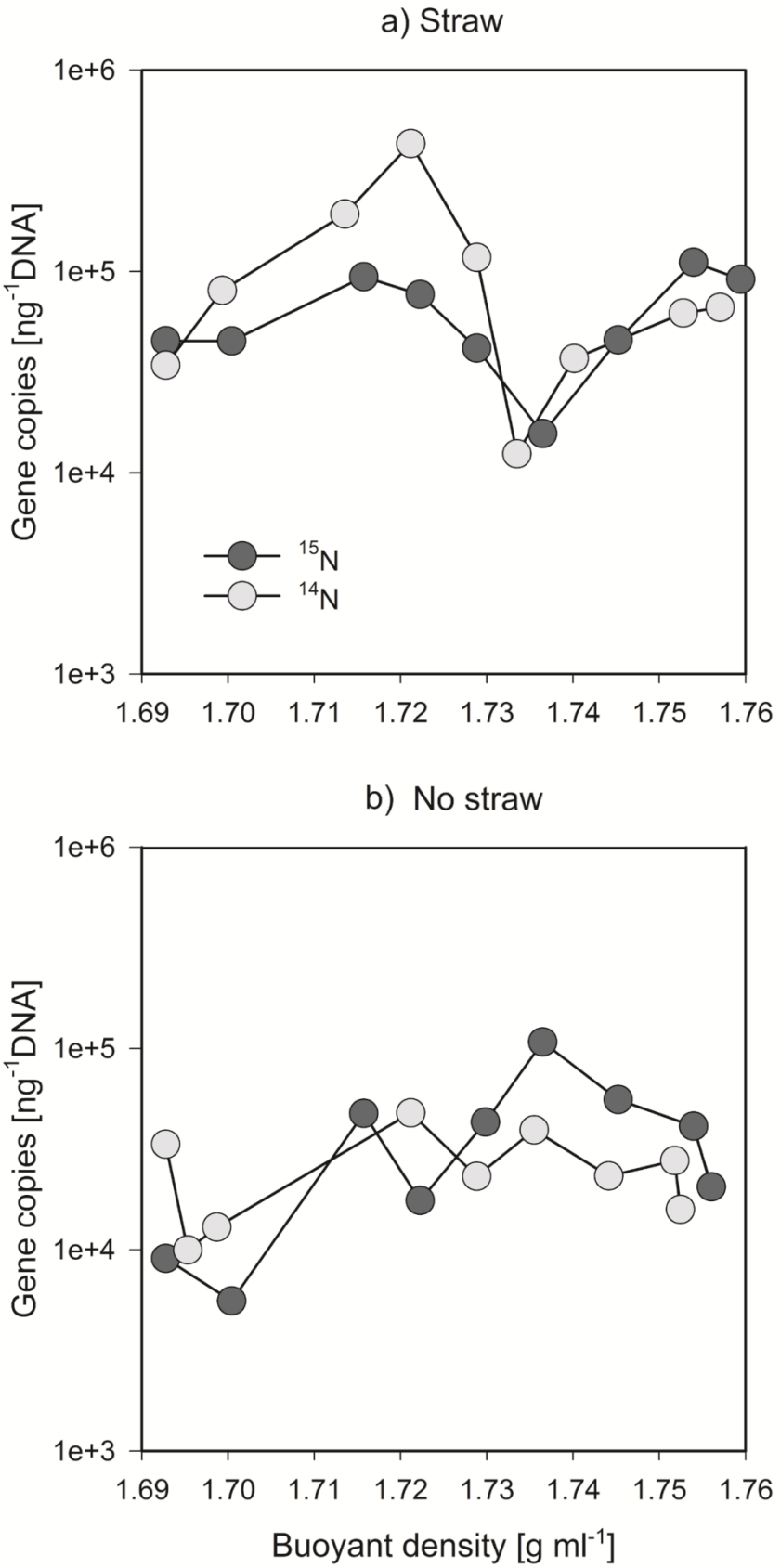
a) Straw
1e+6
1e+5
1e+4
1e+3
Gene copies [ng-1DNA]
15N
14N
1.69
1.70
1.71
1.72
1.73
1.74
1.75
1.76
b) No straw
1e+6
1e+5
1e+4
1e+3
Gene copies [ng-1DNA]
1.69
1.70
1.71
1.72
1.73
1.74
1.75
1.76
Buoyant density [g ml-1]

Figure 8

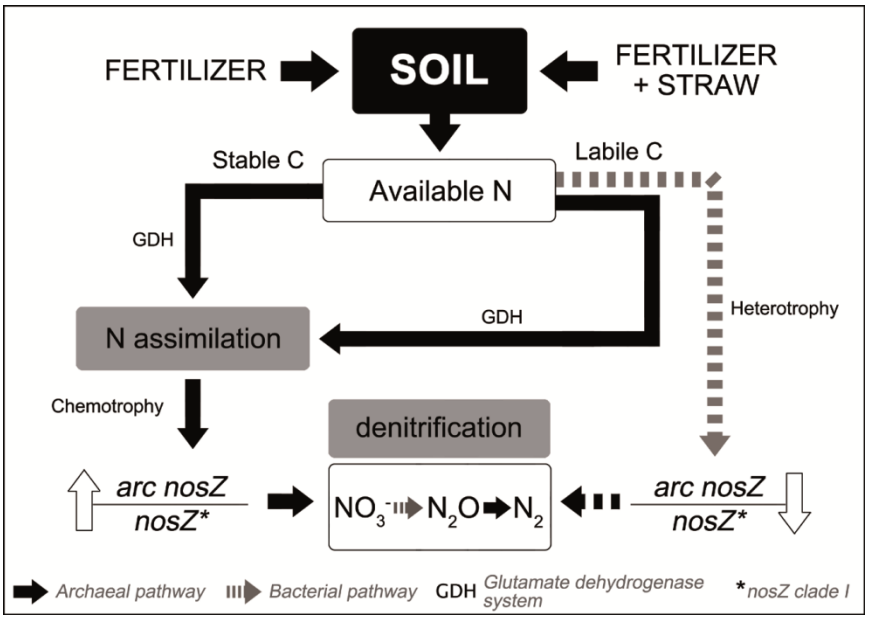
FERTILIZER
SOIL
FERTILIZER + STRAW
Stable C
Available N
Labile C
GDH
GDH
Heterotrophy
N assimilation
Chemotrophy
denitrification
arc nosZ
nosZ*
NO3- N2O N2
arc nosZ
nosZ*
Archaeal pathway
Bacterial pathway
GDH Glutamate dehydrogenase system
*nosZ clade I

Table 1 Description of primer sets and amplification details used for quantitative PCR.

Target group	Primer (reference)	Amplification details
All bacteria (16S rRNA gene)	Eub338 (Lane 1991) Eub518 (Muyzer et al. 1993)	40 cycles 95°C 30s, 55°C 35s, 72°C 45s
All archaea (16S rRNA gene)	Ar109f (Lueders and Friedrich 2000) Ar912r (Lueders and Friedrich 2000)	40 cycles 95°C 30s, 52°C 35s, 72°C 45s, 78°C 20s
nosZ gene clade I	nosZ-2f (Henry et al. 2006) nosZ-2r (Henry et al. 2006)	6 touch down cycles 95°C 15s, 65°C 30s (-1), 72°C 30s 40 cycles 95°C 15s, 60°C 30s, 72°C 30s, 81°C 30s
arc-nosZ gene	arc-Nos-f (Rusch 2013) arc-Nos-r (Rusch 2013)	6 touch down cycles 95°C 15s, 65°C 30s (-1), 72°C 30s 40 cycles 95°C 15s, 60°C 45s, 72°C 60s, 81°C 35s
gdhA gene	MSM0888f (Samuel et al. 2007) MSM0888r (Samuel et al. 2007)	40 cycles 95°C 30s, 58°C 35s, 74°C 30s

Table 2 Description of primer sets, PCR ingredients and amplification details used for T-RFLP analysis.

Target group	Primer (reference)	DNA (ng)	Taq (U)	$MgCl_2$ (mM)	Primer (mM)	dNTPs (mM)	Amplification details
All archaea	Ar109f (Lueders and Friedrich 2000) Ar912r (Lueders and Friedrich 2000)	5	2	1.5	0.15	0.2	35 cycles 95°C 5 m, 95°C 60s, 52°C 30s, 72°C 60s,72°C10 m
nosZ gene clade I	nosZ-2f (Henry et al. 2006) nosZ-2r (Henry et al. 2006)	10	2	1.5	0.2	0.2	6 touch down cycles 94°C 30s, 65°C 30s (-1), 72°C 30s 40cycles 94°C 30s, 60°C 30s, 72°C 30s
arc-nosZ gene	arc-Nos-f (Rusch 2013) arc-Nos-r (Rusch 2013)	10	0.5	-	0.4	0.2	40 cycles 95°C 60s, 95°C 20s, 72°C 20s, 72°C 90s, 72°C 15 m

Table 3 Linear correlation coefficients (Pearson correlation coefficients, n=36) between microbial abundance and chemical data

Property	All bacteria		All archaea		total *nosZ* clade I		*arc-nosZ*		*gdhA*	
	straw	no straw	straw	no straw	straw	no straw	straw	no straw	straw	no straw
NH_4^+	0.351*	0.709***	0.469**	0.879***	0.414*	0.854***	0.457**	0.796***	0.313*	0.706***
TDN	ns	0.593***	ns	0.662***	ns	0.439**	ns	0.550***	0.574***	0.624***
NO_3^-	ns	ns	ns	ns	ns	0.319*	ns	0.272*	ns	ns
DOC	-0.464**	-0.450**	-0.470**	-0.742***	0.153*	0.216*	0.237*	0.246*	ns	-0.427**

Significance levels: not significant-ns: $p>0.05$; *$p<0.05$; **$p<0.01$; ***$p<0.001$.

Table 4 Analysis of similarity (ANOSIM) revealing the treatments effect and time on soil archaeal, total prokaryotic *nosZ* (*nosZ*) clade I and archaeal *nosZ* (arc-*nosZ*) denitrifying community structure

	Global R		
Factor	All archaea	*nosZ* clade I	*arc-nosZ*
straw	ns	0.173***	0.472***
time	0.479***	0.358***	0.567***
straw × time	0.724***	0.691***	0.735***

Levels of significance between two tested populations: not significant-ns: $p>0.05$; ***$p<0.001$.

Highlights

- Archaeal N assimilation was not affected by C availability
- N assimilation and immobilization preceded the archaeal denitrification
- In the presence of labile C denitrifying bacteria outcompeted archaeal counterparts
- Metabolic resilience induced a significant role of archaea in N_2O reduction
- A conceptual model of archaeal assimilatory denitrification was proposed

Supplementary Figure 1

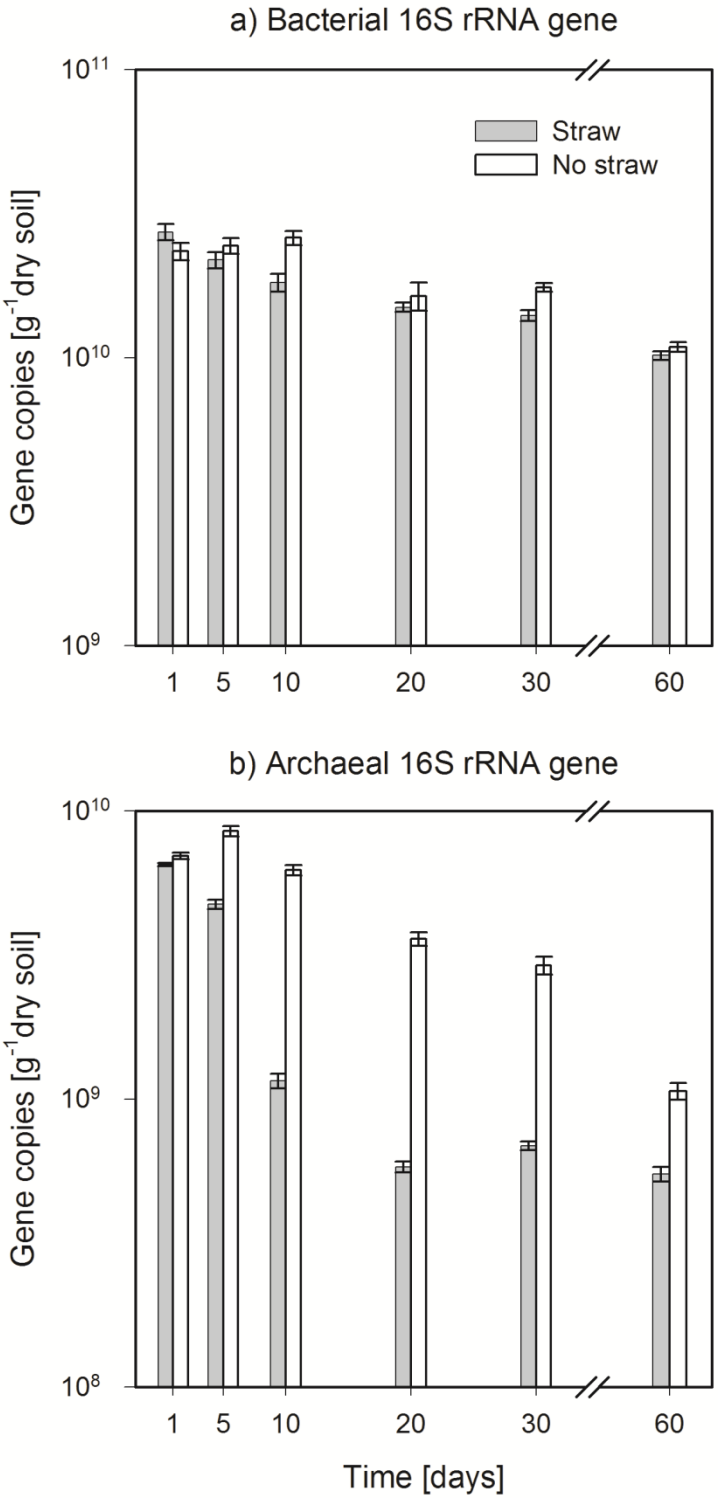

FIG. S1 Abundance of bacterial (a) and archaeal (b) 16S rRNA genes over time in soils incubated with or without straw addition (n=6, means with standard errors).

Supplementary Figure 2

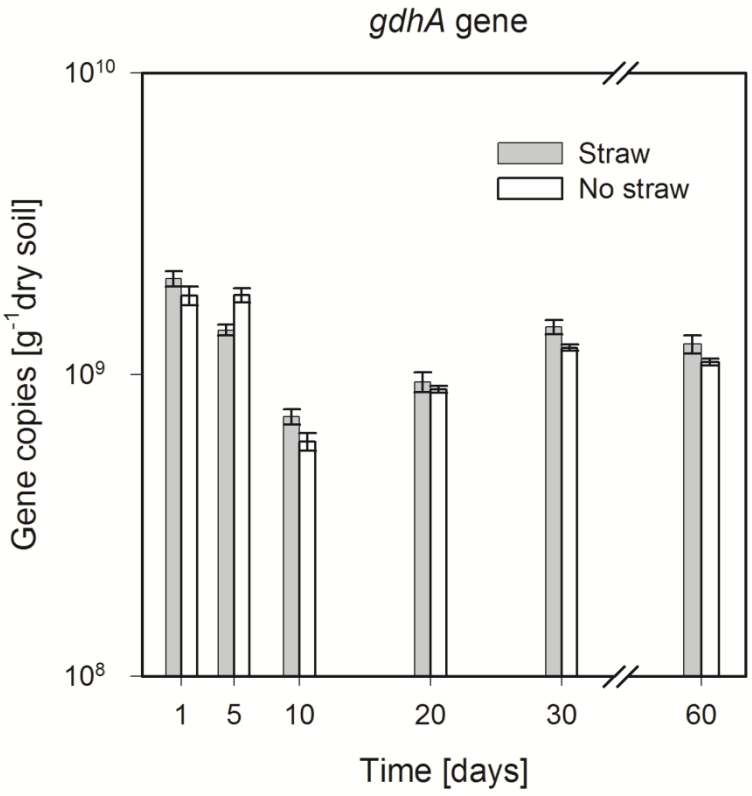

FIG. S2 Abundance of archaeal *gdhA* genes over time in soils incubated with or without straw addition (n=6, means with standard errors).

Supplementary Figure 3

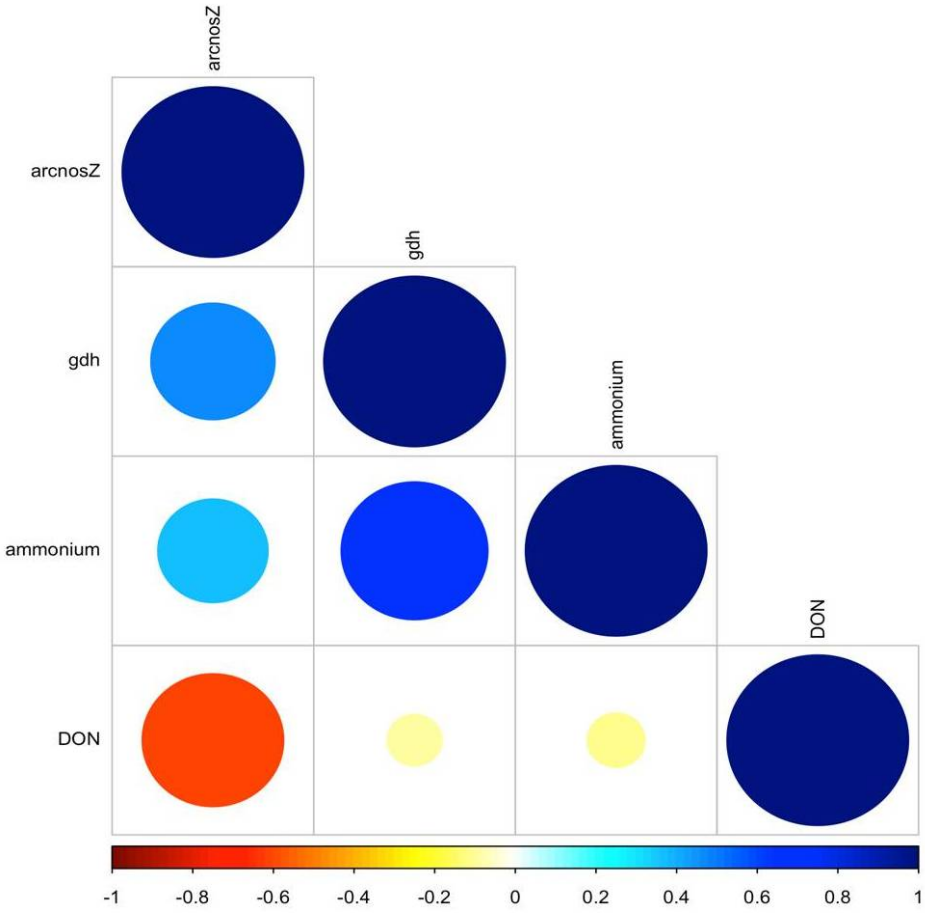

FIG. S3 Significant co-occurrence and co-exclusion relationships between *arc-nosZ* and *gdhA* genes abundances and chemical properties (NH_4^+, DON). Spearman's rank correlation matrix of genes abundance and chemical properties values. Strong correlations are indicated by large circles, whereas weak correlations are indicated by small circles. The colours of the scale bar denote the nature of the correlation, with 1 indicating a perfectly positive correlation (dark blue) and -1 indicating a perfectly negative correlation (dark red). Only significant correlations (FDR < 0.05) are shown.

Supplementary Figure 4

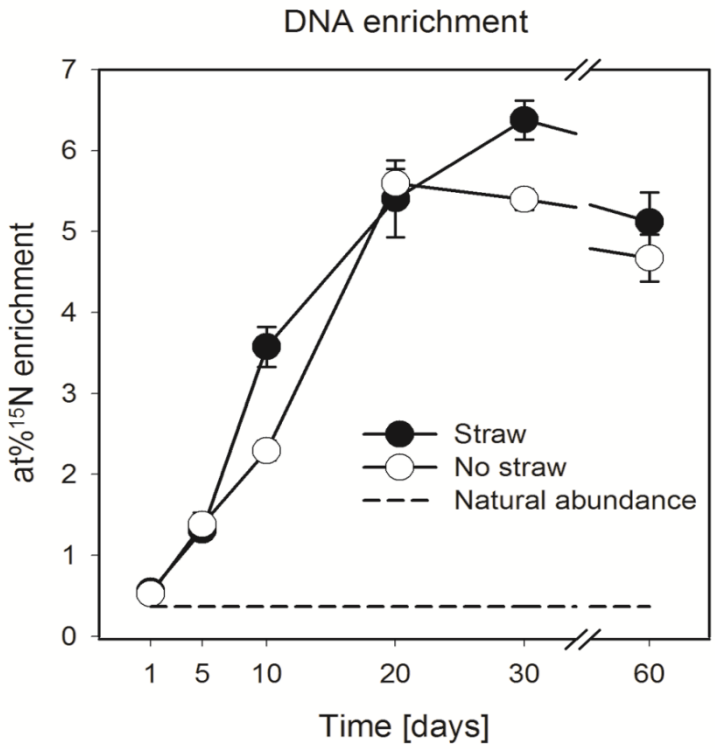

FIG. S4 Development of ^{15}N enrichment of DNA (at% ^{15}N) during incubation time and natural abundance of 0.336 at % ^{15}N of ammonium sulphate (dashed line) (n=3, means with standard errors).